

1 **Responses of field-grown maize to different soil types, water regimes, and** 2 **contrasting vapor pressure deficit**

3 Thuy Huu Nguyen¹, Thomas Gaiser¹, Jan Vanderborcht³, Andrea Schnepf³, Felix Bauer³, Anja
4 Klotzsche³, Lena Lärm³, Hubert Hüging¹, Frank Ewert^{1, 2}

5 ¹University of Bonn, Institute of Crop Science and Resource Conservation (INRES), Katzenburgweg 5, 53115
6 Bonn, Germany

7 ²Leibniz Centre for Agricultural Landscape Research (ZALF), Institute of Landscape Systems Analysis,
8 Eberswalder Strasse 84, 15374 Muencheberg, Germany

9 ³Agrosphere (IBG-3), Institute of Bio- and Geosciences, Forschungszentrum Jülich GmbH, 52428, Jülich,
10 Germany

11 *Corresponding author, email: tngu@uni-bonn.de

12 **Abstracts**

13 Drought is a serious constraint to crop growth and production of important staple crops such as maize.
14 Improved understanding of the responses of crops to drought can be incorporated into cropping system
15 models to support crop breeding, varietal selection and management decisions for minimizing negative
16 impacts. We investigate the impacts of different soil types (stony and silty) and water regimes (irrigated
17 and rainfed) on hydraulic linkages between soil and plant, as well as root: shoot growth characteristics.
18 Our analysis is based on a comprehensive dataset measured along the soil-plant-atmosphere pathway at
19 field scale in two growing seasons (2017, 2018) with contrasting climatic conditions (low and high VPD).
20 Roots were observed mostly in the topsoil (10-20 cm) of the stony soil while more roots were found in the
21 subsoil (60-80 cm) of the silty soil. The difference in root length was pronounced at silking and harvest
22 between the soil types. Total root length was 2.5 - 6 times higher in the silty soil compared to the stony
23 soil with the same water treatment. At silking time, the ratios of root length to shoot biomass in the rainfed

24 plot of the silty soil (F2P2) were 3 times higher than those in the irrigated silty soil (F2P3) while the ratio
25 was similar for two water treatments in the stony soil. With the same water treatment, the ratios of root
26 length to shoot biomass of silty soil was higher than stony soil. The seasonally observed minimum leaf
27 water potential (ψ_{leaf}) varied from around -1.5 MPa in the rainfed plot in 2017 to around -2.5 MPa in the
28 same plot of the stony soil in 2018. In the rainfed plot, the minimum ψ_{leaf} in the stony soil was lower than
29 in silty soil from -2 to -1.5 MPa in 2017, respectively while these were from -2.5 to -2 MPa in 2018,
30 respectively. Leaf water potential, water potential gradients from soil to plant roots, plant hydraulic
31 conductance ($K_{\text{soil_plant}}$), stomatal conductance, transpiration, and photosynthesis were considerably
32 modulated by the soil water content and the conductivity of the rhizosphere. When the stony soil and silt
33 soil are compared, the higher 'stress' due to the lower water availability in the stony soil resulted in less
34 roots with a higher root tissue conductance in the soil with more stress. When comparing the rainfed with
35 the irrigated plot in the silty soil, the higher stress in the rainfed soil resulted in more roots with a lower
36 root tissue conductance in the treatment with more stress. This illustrates that the 'response' to stress can
37 be completely opposite depending on conditions or treatments that lead to the differences in stress that
38 are compared. To respond to water deficit, maize had higher water uptake rate per unit root length and
39 higher root segment conductance in the stony soil than in the silty soil, while the crop reduced transpired
40 water via reduced aboveground plant size. Future improvements of soil-crop models in simulating gas
41 exchange and crop growth should further emphasize the role of soil textures on stomatal function,
42 dynamic root growth, and plant hydraulic system together with aboveground leaf area adjustments.

43 **Key words:** irrigation, plant hydraulic conductance, transpiration, root length, soil types, soil to leaf water
44 potential, stomatal regulation

45 **Abbreviations:** DOY: day of the year; DAS: day after sowing; TUE: transpiration use efficiency; SF: sap flow;
46 LAI: green leaf area index; PAR: photosynthetically active radiation; VPD: vapor pressure deficit; An: net
47 leaf photosynthesis; E: leaf transpiration; ψ_{leaf} : leaf water potential; $\psi_{\text{sunlitleaf}}$: leaf water potential of sunlit

48 leaf; $\psi_{\text{shadedleaf}}$: leaf water potential of shaded leaf; K_{soil} : hydraulic conductance of soil; K_{root} : root hydraulic
49 conductance; K_{stem} : stem hydraulic conductance; $\psi_{\text{soil_effec}}$: effective soil water potential; $\psi_{\text{difference}}$:
50 difference between effective soil water potential and sunlit leaf water potential; $K_{\text{soil_root}}$: root system
51 hydraulic conductance (includes soil and root hydraulic conductance); $K_{\text{soil_plant}}$: whole plant hydraulic
52 conductance (includes below and aboveground components).

53 **1. Introduction**

54 Maize (*Zea mays L.*) is a major staple crop throughout the world. Drought stress, which negatively affects
55 crop growth and yield, is of increasing concern in several important maize cultivating regions (Daryanto et
56 al., 2016). Increases in frequency and severity of drought events due to climate change have been recently
57 reported (IPCC, 2022). Thus, field observations and understanding on how maize responds to water stress
58 are necessary to suggest promising traits for breeding programs (Vadez et al., 2021) as well as irrigation
59 schemes (Fang and Su, 2019; Q. Cai et al., 2017). Improved understanding of crops' response to drought
60 can be incorporated into soil-crop models (e.g. crop modelling and soil-vegetation-atmosphere transfer
61 modelling).

62 Stomatal regulation is often considered as a key aboveground hydraulic variable in regulating water use
63 of crops. Maize is considered as isohydric plant in which stomata are closed in response to sensing drought
64 conditions to maintain leaf water potential (ψ_{leaf}) above critical levels ($\psi_{\text{threshold}}$ or minimum ψ_{leaf}) (Tardieu
65 and Simonneau, 1998). The isohydric behavior is due to different mechanisms including hydraulic and/or
66 chemical (e.g. abscisic acid [ABA]) signals (Tardieu, 2016). The degree to which these underlying
67 mechanisms interact and differ among genotypes and/or environmental scenarios in explaining the
68 stomatal regulation is still debated (Tardieu, 2016; Hochberg et al., 2018). Field evidence in variation of
69 the minimum ψ_{leaf} of maize due to soil water availability and soil hydraulics is rarely reported.

70 Water flow along the soil-plant-atmosphere continuum is determined by a series of hydraulic
71 conductivities and gradients in water potential. Hydraulic conductance of soil (K_{soil}), root hydraulic

72 conductance (K_{root}), and stem hydraulic conductance (K_{stem}) determine water potential from soil to root
73 and root xylem water, and thus magnitude of ψ_{leaf} . There are two main resistances to water flow from the
74 soil to the shoot, namely the soil and the root resistances, often expressed as their inverse, K_{soil} and K_{root}
75 (Nguyen et al., 2020; Cai et al., 2018). In wet soils, the soil hydraulic conductivity is much higher than that
76 of roots, and water flow is mainly controlled by root hydraulic conductivity (Hopmans and Bristow, 2002;
77 Draye et al., 2010). It is well-known that a decrease in soil matric potential and soil hydraulic conductivity
78 triggers stomatal closure and thus results in reduction in transpiration rate (Sinclair and Ludlow, 1986;
79 Carminati and Javaux 2020; Abdalla et al., 2021). For the root water uptake and controlling stomata, the
80 location where soil and roots are in close contact (rhizosphere) is most important, because when this thin
81 layer of rhizosphere is disconnected (i.e. soil-root contact is lost), the water movement from soil toward
82 the roots is reduced, which might trigger stomatal closure to maintain hydraulic integrity of plant
83 (Carminati et al., 2016; Rodriguez-Dominguez and Brodribb, 2019; Abdalla et al., 2022). The magnitude of
84 the drop of water potential between bulk soil and soil-root interface increases considerably at different
85 levels of soil dryness for different soil types (Carminati and Javaux, 2020; Abdalla et al., 2022). Hydraulic
86 limits in the soil (Carminati and Javaux, 2020), or in the root–soil interface [as measured for olive trees by
87 Rodriguez-Dominguez and Brodribb, 2019 or tomato (Abdalla et al., 2022)], or in the root properties
88 (Bourbia et al., 2021; Cai et al., 2022; Nguyen et al., 2020; Cai et al., 2018) or due to both soil textures and
89 root phenotypes (Cai et al., 2022b) emphasized the importance of belowground hydraulics (Carminati and
90 Javaux, 2020). However, also the shoot hydraulic conductance could be limiting in some crop plants
91 (Gallardo et al., 1996) or in trees (Domec and Pruyn, 2008; Tsuda and Tyree, 1997). Stomatal conductance
92 and shoot hydraulic conductance showed close links to each other in pine trees (Hubbard et al., 2001).
93 This summary illustrates three points: (i) current studies have often focused either on above or on below
94 hydraulic limits, but rarely consider both (ii) it is unclear the roles and relations of soil hydraulic properties
95 to root and plant hydraulic conductance (thus influences on stomatal conductance) (iii) the role of different

96 hydraulic processes across the soil - plant - atmosphere continuum i.e. soil to roots, stem, and soil-plant
97 hydraulic conductance in controlling stomatal conductance remains unclear.

98 Simultaneous measurements of atmospheric conditions (light intensity and vapor pressure deficit), leaf
99 water potential, and transpiration rates, coupled with measurements of root, stem and whole soil-plant
100 hydraulic conductance, root architecture, and soil water potential distribution could reveal the relative
101 importance of rhizosphere, shoot and root growth, and hydraulic conductance vulnerability, especially
102 under progressive soil drying at field conditions (Carminati and Javaux, 2020; Tardieu et al., 2017). For the
103 soil water conditions, soil texture and hydraulic characteristics are very important because they influence
104 soil water movement and thus affect infiltration, surface and sub-surface runoff, and ultimately plant
105 available soil water (Vereecken et al., 2016). Soil texture properties, characterized by different fractions of
106 clay, silt, and sand particles, are important drivers in determining the soil water retention properties
107 (Scharwies and Dinneny, 2019; Stadler et al., 2015; Zhuang et al., 2001). Soil with higher water holding
108 capacity (here the silty soil with low stone content) have a larger amount of plant available water which in
109 turn enables crops to better meet the evaporative demand and facilitates better crop growth as compared
110 to the soil with high stone content (Nguyen et al., 2020; Cai et al., 2018). Estimations of hydraulic
111 conductance (different organs and whole plant hydraulic conductance) were done for crop plants and
112 maize mainly under controlled environment or pot conditions e.g. for different species and genotypes
113 during soil drying (Sunita et al., 2014; Choudhary and Sinclair, 2014; Abdalla et al., 2022; Meunier et al.,
114 2018; Wang et al., 2017; Li et al., 2016) or various species and genotypes together with different soil
115 textures (Cai et al., 2022a), or soil texture with different vapor pressure deficit (VPD) (Cai et al., 2022b).
116 Compared to the substantial effect of soil texture, there was no evidence of an effect of VPD on both soil-
117 plant hydraulic conductance and on the relation between canopy stomatal conductance and soil-plant
118 hydraulic conductance in pot-grown maize (Cai et al., 2022b). Contrast results were found in winter wheat
119 where plant hydraulic conductance increased with rising VPD for some genotypes in wet conditions

120 (Ranawana et al., 2021). Vadez et al., (2021) examined the effects of soil types together with increasing
121 VPD on transpiration efficiency (TE) and yield under pot conditions for several C₄ species (maize, sorghum,
122 and millet). The interpretation of differences in TE was attributed to soil types, more specifically, to the
123 differences in soil hydraulic properties and soil hydraulic conductance. However, experimental evidence
124 linking root hydraulics to stomatal regulation was lacking in these two Vadez's studies (Vadez et al., 2021).
125 Recent field studies have aimed at quantification of root hydraulic conductance and its linkages with crop
126 growth (leaf area and biomass) under different soil types (in wheat Cai et al., 2017; Cai et al., 2018; Nguyen
127 et al., 2020 or maize in Nguyen et al., 2022; Jorda et al., 2022). However, field studies that consider both
128 below (soil-root hydraulic conductance) and above (stem hydraulic conductance), or soil-plant hydraulic
129 conductance (including below and above-ground parts) and their roles in stomatal regulation as well as
130 crop growth (leaf area and biomass) are rarely carried out.

131 This study aims at further understanding of the hydraulic linkages between soil and plant and responses
132 of plants to drought stress in relation to root: shoot growth characteristics at field scale. We hypothesize
133 that, in field-grown maize, (1) soil-plant hydraulic conductance depends on soil hydraulic properties,
134 especially under dry soil conditions (2) minimum leaf water potential of maize is similar across soil types,
135 water treatments and climatic conditions. The hypotheses will be tested through three objectives: (i) to
136 investigate the effects of soil types, water application, and climatic condition on root growth and (ii) on
137 stomatal conductance, leaf photosynthesis, transpiration, leaf water potential, different components of
138 the hydraulic conductance (root, stem, and whole soil-plant), and (iii) to analyze the relative contribution
139 of root and shoot growth (leaf area and biomass) on the water uptake capacity of maize. These three
140 objectives will be achieved based on a comprehensive dataset covering the whole soil-plant continuum
141 over two growing maize seasons with contrasting climatic conditions (low and high VPD) under two water
142 treatments (rainfed and irrigated) and two different soil types (stony and silty soil).

143

144 **2. Materials and methods**

145 **2.1. Location and experimental set-up**

146 We carried out a field experiment at two rhizotron facilities in Selhausen, North Rhine-Westphalia,
147 Germany (50°52'N, 6°27'E). The field is slightly inclined with a maximum slope of around 4°. One rhizotrone
148 facility was located upslope (F1) with around 60% gravel by weight in the 10-cm topsoil while the second
149 rhizotrone facility was at downslope (F2) with silty soil (stone content is around 4% by weight).

150 Each rhizotrone facility was divided into three subplots of 7.25 m by 3.25 m: two rainfed plots (P1, P2),
151 and one irrigated plot (P3). In rainfed plots P1, other sowing densities and dates were used than in the
152 other plots and we excluded therefore these plots. Silage maize cv. Zoey was sown on 4 May and 8 May in
153 2017 and 2018, respectively, with a plant density of 10.66 seeds m⁻² (Figure 1a; Table 1). Detailed
154 information of crop management practices is provided in Table 1.

155 [Insert Table 1 here]

156 **2.2. Water applications**

157 Weather variables (global radiation, temperature, relative humidity, precipitation, and wind speed) were
158 recorded every 10 minutes by a nearby weather station (approx. 100 m from the experiment). Drip lines
159 (T-Tape 520-20-500, Wurzelwasser GbR, Müzenberg, Germany) were installed for irrigation at 0.3 m
160 intervals parallel to the crop rows. In 2017, maize received a total amount of 230 mm precipitation during
161 the growing period (136 days). Average, minimum and maximum daily air temperature were 17.6, 8.3, and
162 25.3 °C, respectively (Fig. 1b). The crop on P3 was irrigated (in total 130 mm) every 5-7 days (in total 10
163 times) using 13 mm of irrigation water per event between mid June to end of August for the irrigated plots
164 (2017F1P3 and 2017F2P3) (Fig. 1b). In 2018, average, minimum, and maximum daily air temperature were
165 19.2, 10.85, and 27.3 °C, respectively (Fig. 1b) and exceeded those of 2017. Characterized by exceptionally
166 hot and dry weather conditions, the summer season 2018 can be classified as an extreme year with respect
167 to plant growth at our experimental location. Maize experienced high temperatures and VPD, especially

168 around tasseling and silking. In 2018, only 91.3 mm of rain were recorded in the growing period of 2018
169 (107 days). The maize crop was irrigated every 5-7 days (in total 13 times), with a total amount of irrigation
170 of 257 mm and 239 mm between mid- June and mid- August for the irrigated plots 2018F1P3 and
171 2018F2P3, respectively (Fig. 1d). In contrast to 2017, the rainfed plot in the stony soil (2018F1P2) had to
172 be irrigated (in total 66 mm) four times (using 13, 22, 13, and 18 mm, respectively) to avoid a crop failure
173 due to severe drought (Fig. 1d). Detailed estimates of irrigation amount and intervals could be found in
174 Nguyen et al., (2022a).

175 [Insert Figure 1 here]

176 **2.3. Measurements**

177 **2.3.1. Soil water measurement and root growth**

178 At soil depths of 10, 20, 40, 60, 80, and 120 cm, MPS-2 matrix water potential and temperature sensors
179 (Decagon Devices Inc., UMS GmbH München, Germany) were installed to measure half-hourly soil water
180 potential and soil temperature. The range of the water potential measurements is from -9 kPa to
181 approximately -100000 kPa (pF 1.96 to pF 6.01). In addition to MPS-2, soil water potential was measured
182 by pressure transducer tensiometers (T4e, UMS GmbH, München, Germany) where the minimum
183 detectable suction is -85 kPa to +100 kPa. A detailed description of sensor installation, calibration and data
184 post processing can be found in Cai et al., (2016).

185 Minirhizotubes (7 m long clear acrylic glass tubes with outer and inner diameters of 6.4 and 5.6 cm,
186 respectively) were installed horizontally at six different depths of 10, 20, 40, 60, 80, and 120 cm below the
187 soil surface in each facility. There are three replicate tubes at each depth, accounting for 54 tubes in each
188 facility. Root measurements were taken manually by Bartz camera (Bartz Technology Corporation) (23
189 June 2017 – 12 September 2017) and VSI camera (Vienna Scientific Instruments GmbH) (08 June 2017 – 22
190 June 2017) in 2017 while only VSI was used in 2018 (23 May 2018 - 23 August 2018). Root images were

191 taken at 20 fixed positions from the left- and right-hand sides of each tube weekly (or biweekly) during the
192 growing seasons. The root images were analyzed by automated minirhizotube image analysis pipeline for
193 segmentation and automated feature extraction (Bauer et al., 2021). Two-dimensional root length density
194 (RLD, in units of cm cm^{-2}) was estimated from the total root length observed in the image and the image
195 surface area. The overview of camera system, minirhizotube images acquisition, and post-processing of
196 the root data were described in detail in Bauer et al. (2021) and Lärm et al., (2023).

197 **2.3.2. Crop growth, leaf gas exchange, leaf water potential, and sap flow measurements**

198 The phenology, plant height, stem diameter, green and brown leaf area, dry matter of different organs,
199 and total aboveground dry matter were observed and measured bi-weekly. Dates of sowing, emerge,
200 tasseling, and silking for two growing seasons were observed. There was difference in emerge, tasseling
201 and silking dates for two growing seasons due to the differences of sowing dates and temperature.
202 However, the developmental stages were not different among water treatments and soil types within one
203 season. Measurements of green leaf area and aboveground dry matter were based on the destructive
204 method.

205 Hourly leaf stomatal conductance (G_s), net photosynthesis (A_n), and leaf transpiration (E) were measured
206 every two weeks under clear sky conditions. The G_s , A_n , and E of two sunlit leaves (uppermost fully
207 developed leaves) and one shaded leaf of different plants were measured at steady-state using a LICOR
208 6400 XT device (Licor Biosciences, Lincoln, Nebraska, USA). Leaf water potential (ψ_{leaf}) was measured with
209 a pressure chamber (SKPM 140/ (40-50-80), Skye Instrument Ltd, UK).

210 In 2017 (from 7 July 2017 until harvest) and 2018 (from 28 June 2018 until harvest), 20 sap flow sensors
211 (SGA 13, SGB 16, and SGB 19 types) were installed (one sensor per plant and 5 maize plants per plot) based
212 on stem diameter size. The sap flow in the plant (g h^{-1}) was estimated directly by the data loggers

213 (Dynamax, 2007) and used as a surrogate for canopy transpiration based on the number of plants per
 214 square meter. Further detail of developmental stages, crop growth, leaf gas exchange, leaf water potential,
 215 and sap flow measurements could be found in Nguyen et al., (2022a) and Nguyen et al., (2020).

216 **2.4. Calculation of total root length, root system conductance, stem, and whole plant hydraulic**
 217 **conductance**

218 To estimate the total root length from minirhizotubes, we adopted the option 2 which was described in
 219 Cai et al., (2017). Total root length per square meter soil surface area within each soil layer ($m\ m^{-2}$) was
 220 computed by multiplying the root length density with the corresponding soil layer thickness. The root
 221 length density was determined in each depth by dividing the measured root length per minirhizotron
 222 image by the assumed volume the roots would have occupied in absence of the tube, i.e., $W * L * tube$
 223 radius (see Cai et al., 2017).

224 Following Nguyen et al., (2020), the effective soil water potential was calculated based on hourly measured
 225 soil water potential (ψ_i) and normalized root length density at six depths (10, 20, 40, 60, 80, and 120 cm)
 226 ($NRLD_i$), and soil layer thickness (Δz_i) in the soil profile (Equation 1).

$$\psi_{soil_efec} = \sum_{i=1}^N \psi_i NRLD_i \Delta z_i \quad (1)$$

227 We followed Ohm's law analogy by dividing the hourly sap flow by the difference between effective soil
 228 water potential and shaded leaf water potential to estimate root system conductance (K_{soil_root} - Equation
 229 2), between shaded leaf water potential and sunlit leaf water potential to estimate stem hydraulic
 230 conductance (K_{stem} - Equation 3), and between effective soil water potential and sunlit leaf water potential
 231 to estimate whole plant hydraulic conductance (K_{soil_plant} - Equation 4).

$$K_{soil_root} = Sapflow / (\psi_{soil_efec} - \psi_{shadedleaf}) \quad (2)$$

$$K_{stem} = Sapflow / (\psi_{shadedleaf} - \psi_{sunlitleaf}) \quad (3)$$

$$K_{soil_plant} = Sapflow / (\psi_{soil_effec} - \psi_{sunlitleaf}) \quad (4)$$

232 During one measurement day, four values of the K_{soil_root} , K_{stem} , and K_{soil_plant} were obtained from
233 measurements between 11AM and 2 PM. The average and standard deviation of these hourly
234 measurements were calculated for each measurement day in order to present the seasonal dynamics of
235 those variables. To capture the diurnal and seasonal variations of sap flow and sunlit leaf water potential,
236 in addition, we plotted the hourly sap flow and hourly difference of effective soil water potential and sunlit
237 leaf water potential for three measurement days starting from predawn and whole seasons, respectively,
238 to derive the slope which is also K_{soil_plant} .

239 2.5. Statistical analysis

240
241 Regression analysis was performed to understand the relationship between the sap flow volume and the
242 difference of effective soil water potential and sunlit leaf water potential as well as the relationship
243 between the total aboveground biomass and cumulated water transpired (sap flow volume). These
244 analyses allow to derive the slope as proxy of K_{soil_plant} and transpiration use efficiency, respectively. Since
245 all measured data have their own measurement errors, the generalized Deming regression was employed.
246 We performed relationships (via correlation coefficient and statistical significant levels) of midday leaf A_n ,
247 G_s , and E with midday K_{stem} , K_{soil_plant} , K_{soil_root} , sunlit leaf potential, ψ_{soil_effec} , and the difference of ψ_{soil_effec}
248 and sunlit leaf water potential ($\psi_{difference}$). All data processing and analysis were conducted using the R
249 statistical software (R Core Team, 2022).

250 3. Results

251 3.1. Root growth under different water treatments, soil types and climatic conditions

252 Observed root length ($cm\ cm^{-2}$) from the minirhizotubes in different soil depths at the first week of June
253 (stem elongation), around silking, and at harvest in two growing seasons are shown in the Figure 2. Root

254 length was similar among water treatments at the start of stem elongation in both years (Fig. 2a & 2d).
255 The difference in root length was pronounced at silking and harvest between the soil types. More root
256 growth was observed in the silty soil compared to the stony soil with the same water treatment (i.e. 2.5 -
257 6 times higher at depth 40 cm). This indicated the strong negative effects of stone content on root
258 development. In the stony soil, root length in the irrigated plot (F1P3) was slightly higher than in the rainfed
259 plot (F1P2). In contrast, the rainfed treatment (F2P2) in the silty soil showed much higher root length,
260 especially from 40 to 120 cm depths as compared to the irrigated plot (F2P3) in both growing seasons.
261 Much lower stone content and deep soil cracks in the silty soil (Morandage et al., 2021) allow root
262 extension to the subsoil, particularly in the rainfed plot F2P2. Root length in the rainfed treatment (F2P2)
263 in 2018, is higher than in 2017 which implies that root further developed to exploit the water in the soil
264 under the rainfed condition to meet the higher evaporative demand.

265 [Insert Figure 2 here]

266 Total root length (m m^{-2}) estimated from minirhizotubes and its ratio to shoot dry matter (m kg^{-1}) at three
267 measured dates (as in Figure 2) are shown in the Figure 3. Total root length was much higher for the silty
268 plots as compared to stony plots. In 2017, the highest total root length was observed in the rainfed plot of
269 the silty soil (F2P2) with approximately 9166 m m^{-2} and 9878 m m^{-2} around silking and harvest, respectively,
270 which was almost two times higher than in the irrigated plot (F2P3). These figures were higher in 2018
271 than 2017 where total root length of F2P2 was 10188 m m^{-2} and 13750 m m^{-2} at silking and harvest time,
272 respectively. For the rainfed stony soil (F1P2), soil water depletion around the beginning of June in 2017
273 (Supplementary material 1a) and from the first two weeks of June to harvest in 2018 (Supplementary
274 material 2a) caused the strong reduction of shoot biomass. In the stony soil, the shoot dry matter of the
275 irrigated plot (F1P3) and the rainfed plot (F1P2) were 1275 and 536 g m^{-2} at silking time (e.g. 19 July 2018
276 – DOY 200, Supplementary material 3a and 3b). However, there was a minor difference between F1P2 and
277 F1P3 in terms of the ratio of root length to shoot dry matter. In the silty soil, a decrease of soil water

278 potential was not pronounced (compared to stony soil) in both years 2017 and 2018 (Supplementary
279 material 1b and 2b). In 2018, shoot biomass in the irrigated stony soil (F1P3) and silt soil (F2P3) were
280 similar (1275 and 1299 g m⁻², respectively on 19 July 2018 – DOY 200) while the shoot biomass of the
281 rainfed silty soil (F2P2) was 876 g m⁻² (Supplementary material 3a & 3b). However, the ratios of root length
282 to shoot biomass in the rainfed plot of the silty soil (F2P2) were 3 and 6 times higher than those in the
283 irrigated silty soil (F2P3) and stony soil (F1P3), respectively (e.g. 18 July, DOY 199). Moreover, total root
284 length was relatively equal among treatments at the start of set elongation (8 June - DOY 159) in both
285 years, while this was the opposite for the ratio of root length to shoot dry matter. This firstly illustrated
286 that the finer soil texture without stones and with soil cracks could favor the root growth which indicates
287 strong interactions of root and soil conditions. Secondly, the larger root length and higher atmospheric
288 evaporative demand in 2018 than 2017 indicates also the interaction of root growth and climatic
289 conditions.

290 [Insert Figure 3 here]

291 **3.2. Stomatal conductance, photosynthesis, transpiration, and $K_{\text{soil_plant}}$**

292 **3.2.1. Diurnal course of stomatal conductance, photosynthesis, transpiration, and water potential at leaf** 293 **level**

294 After a long period with high temperatures and no rainfall, soil water reduction in the rainfed plot of the
295 stony soil (F1P2) on 17 July 2018 (Supplementary material 2) resulted in three times lower net
296 photosynthesis (A_n), stomatal conductance (G_s), transpiration (E) and leaf water potential (ψ_{leaf}) as
297 compared to the remaining treatments (Supplementary material 4). This indicates that the soil water
298 content strongly affected the stomatal conductance. Stomatal closure was much pronounced around
299 midday in F1P2 while this was not the case in the F2P2, indicating the soil type strongly affected the
300 stomatal conductance and leaf gas exchange. Leaf gas exchange and leaf water potential in the F1P2 were
301 still much lower than in other plots (Figure 4). On 18 July 2018, after application of 22.75 mm of irrigation

302 water (at 4 PM), photosynthesis, stomatal conductance, transpiration and leaf water potential were
303 slightly increased in F1P2. However, these were still smaller than in F2P2 and the two irrigated plots.

304 [Insert Figure 4 here]

305 On the next day after irrigation, leaf gas exchange and water potential were considerably increased in the
306 F1P2 (Supplementary material 5). Leaf curling was also less pronounced as compared the two previous
307 days. This indicated the recovery of plant after watering. Leaf water potential, photosynthesis, stomatal
308 conductance, and leaf transpiration were almost similar to other plots from predawn throughout the day.

309 **3.2.2. Seasonal course of stomatal conductance, photosynthesis, transpiration, water potential, and** 310 **plant hydraulic conductance at the leaf level**

311 Seasonal stomatal conductance (G_s) and leaf water potential (ψ_{leaf}) are described in Figure 5. The
312 relationship between two variables was rather noisy and non-linear. The leaf water potential showed
313 distinct patterns among treatments in one growing season. Minimum ψ_{leaf} was maintained at around -1.5
314 MPa in the irrigated plot in stony soil (F1P3) and two plots in the silty soil (F2P2 and F2P3). Lower minimum
315 ψ_{leaf} could be observed in the rainfed plot with stony soil (F1P2) but it did not go beyond -2 MPa. Minor
316 leaf curling was observed only in the second week of June in the F1P2 in 2017. In 2018, the higher
317 temperature and vapor pressure deficit resulted in lower minimum ψ_{leaf} in all treatments and soil types as
318 compared to 2017. The minimum ψ_{leaf} was around -2 MPa in F1P3, F2P2, and F2P3 while ψ_{leaf} could drop
319 below -2 MPa in F1P2 which was due to the severe soil water deficit. The low G_s and ψ_{leaf} associated with
320 measurement dates when the substantial leaf curling was observed at mid of July to the end of growing
321 season in F1P2 in 2018 (Supplementary material 3c & 3d and Supplementary material 6c & d).

322 [Insert Figure 5 here]

323 The effective soil water potential ($\psi_{\text{soil_effect MD}}$), sunlit leaf water potential ($\psi_{\text{sunlitleaf MD}}$), stomatal
324 conductance (G_{sMD}), and whole plant hydraulic conductance ($K_{\text{soil_plant MD}}$) at midday at several times during

325 the growing season are presented in Figures 6 and 7 for 2017 and 2018, respectively. As expected, there
326 was not much difference in terms of $\psi_{\text{soil_effecMD}}$ among F1P3, F2P2, and F2P3 from 02 August to one week
327 before harvest in 2017. The lowest $\psi_{\text{soil_effecMD}}$ was observed in the F1P2. Leaf water potential dropped
328 drastically but also $K_{\text{soil_plantMD}}$ increased strongly whereas $\psi_{\text{soil_effecMD}}$ remained quite similar (e.g. 18 July).
329 This is because sap flow have increased substantially in this day (e.g. from 2.34 mm d⁻¹ on 17 July to 6.97
330 mm d⁻¹ on 18 July for the F1P2). The stomatal conductance decreased a lot in this day which could be
331 explained that the atmospheric demand increased (e.g. global radiation was 13.6 MJ m⁻² on 17 July
332 compared to 23.9 MJ on 18 July while daily VPD was 0.7 kPa and 1.2 kPa, respectively) even more than the
333 sap flow. Midday sunlit leaf water potential was not distinctively different among treatments with the
334 lowest $\psi_{\text{sunlitleafMD}}$ around -1.6 MPa throughout season. Also, G_{SMD} was rather similar among plots. The
335 $K_{\text{soil_plantMD}}$ ranged from 0.125 to 0.96 mm h⁻¹ MPa⁻¹ with a sharp reduction before harvest. In general, the
336 lowest values of $K_{\text{soil_plantMD}}$ were found in F1P2 which was consistent with the smaller overall seasonal
337 $K_{\text{soil_plant}}$ (as the slope of linear relationship between sap flow and difference of effective soil water potential
338 and sunlit leaf water potential) (see Supplementary material 7).

339 [Insert Figure 6 here]

340 The $\psi_{\text{soil_effecMD}}$ was substantially different in the two soil types and water treatments in 2018 (Figure 7a).
341 Both F1P2 and F1P3 showed a gradual drop of $\psi_{\text{soil_effecMD}}$ from 15 June until the third week of July then
342 increased after irrigation events on 18 July (Supplementary material 2b). However, $\psi_{\text{soil_effecMD}}$ of F1P2 was
343 much lower than F1P3 toward the harvest. The $\psi_{\text{soil_effecMD}}$ of F2P2 and F2P3 only decreased progressively
344 from around 10 July till harvest even though there was water supply from the irrigation (Supplementary
345 material 2b). The water applied by irrigation and coming in by rainfall were insufficient to wet up the
346 deeper soil layers which remained dry. The low G_{SMD} was corresponding to the lowest $\psi_{\text{sunlitleafMD}}$ and
347 $K_{\text{soil_plantMD}}$ from the F1P2 (Figure 7c & 7d). The $K_{\text{soil_plantMD}}$ from all plots was ranging from 0.12 to 0.91 mm
348 h⁻¹ MPa⁻¹. There was the drop in $K_{\text{soil_plantMD}}$ (i.e. 3 to 9 July or 17-18 July) before irrigation in this plot.

349 However, it increased after the irrigation (i.e. 10 July and 19 July). This suggests that $K_{\text{soil_plant}}$ depends
350 strongly on the soil water content and the conductivity of the rhizosphere.

351 [Insert Figure 7 here]

352 **3.2.3. Relationships of stomatal conductance, transpiration, photosynthesis with plant hydraulic** 353 **variables at the plant canopy level**

354 The slope of linear relationship between sap flow and difference of $\psi_{\text{soil_effec}}$ and $\psi_{\text{sunlitleaf}}$ is shown for three
355 consecutive days (leaf water potential measurements from the predawn) and before and after irrigation
356 applications (17, 18, and 19 July 2018) (Figure 8). On both dates 17 and 18 July, the difference between
357 $\psi_{\text{soil_effec}}$ and $\psi_{\text{sunlitleaf}}$ was around -1.6 MPa with very low transpiration rates in the treatment F1P2 which
358 was associated with very low plant hydraulic conductance and leaf curling. The whole plant hydraulic
359 conductance was disrupted on these two days (0.06 and $0.16 \text{ mm h}^{-1} \text{ MPa}^{-1}$ for 17 and 18 July, respectively).
360 Water was supplied on 18 July at 1 PM for the irrigated plots (F1P3, F2P3) as well as F1P2 at 4 PM (for
361 saving plant from death due to severe drought stress). $K_{\text{soil_plant}}$ was slightly changed (0.43 and 0.57 mm h^{-1}
362 MPa^{-1} for F1P3 on 18 and 19 July, respectively and 0.5 and $0.58 \text{ mm h}^{-1} \text{ MPa}^{-1}$ for F2P3 on 18 and 19 July,
363 respectively). However, the increase of $K_{\text{soil_plant}}$ was substantial in the F1P2 after the irrigation. Soil water
364 replenishment and an increase in the root - soil contact (Fig. 7a) allowed the $K_{\text{soil_plant}}$ to recover overnight
365 to $0.46 \text{ mm h}^{-1} \text{ MPa}^{-1}$. This resulted in a narrower water potential gradient between root zone and sunlit
366 leaf and in a higher transpiration rate on 19 July.

367 [Insert Figure 8 here]

368 Seasonal average of different midday hydraulic conductance components (root system hydraulic
369 conductance - $K_{\text{soil_root}}$, stem hydraulic conductance - K_{stem} , and whole plant hydraulic conductance -
370 $K_{\text{soil_plant}}$) are shown in Figure 9. In the same year, the K_{stem} was not much different among F1P3, F2P2, and
371 F2P3 plots. The K_{stem} of those plots was slightly higher than in the F1P2 in both years. In general, the $K_{\text{soil_root}}$

372 was lower than the K_{stem} . Overall, the estimated $K_{\text{soil_plant}}$ was around $1 / (1/K_{\text{soil_root}} + 1/K_{\text{stem}})$ regardless of
373 soil types, years, and water treatments. The $K_{\text{soil_root}}$ and $K_{\text{soil_plant}}$ in the F1P2 in 2018 was much lower than
374 the remaining plots while the $K_{\text{soil_root}}$ and $K_{\text{soil_plant}}$ were not much different among plots in 2017. Our results
375 indicated that there was an impact of soil hydraulic conductance on $K_{\text{soil_root}}$ and $K_{\text{soil_plant}}$. Although there is
376 a large difference in total root length between the two soil types (e.g. F1P3 versus F2P2 or F2P3 versus
377 F2P2), $K_{\text{soil_root}}$ and $K_{\text{soil_plant}}$ in those two plots were not much different. This could be explained by the fact
378 that $K_{\text{soil_plant}}$ was not only depended on root length but also depended on the variability of root segment
379 hydraulic conductance.

380 [Insert Figure 9 here]

381 **3.3. Relative importance of root and leaf area growth to transpiration and crop performance at canopy** 382 **level**

383 Drought stress was observed in the rainfed plot (F2P2) in the second week of June 2017 with mild leaf
384 rolling. The crop then recovered due to sufficient rainfall and lower evaporative demand. Drought stress
385 occurring again at the stem elongation phase caused reduction of plant size (height and stem diameter)
386 (Supplementary material 6) as well as a slight reduction of leaf area and biomass in this plot
387 (Supplementary material 3a & 3c). Transpiration per unit of leaf area did not differ much among water
388 treatments and soil types in 2017 (Supplementary material S8). The opposite was the case for the
389 transpiration rate per unit of root length. The observed root length at different soil depths (Figure 2) and
390 total root length for two plots in the stony soil was much smaller than in the silty soil (Figure 3). Therefore,
391 transpiration per unit of root length in the stony soils (F1P2 & F1P3) was almost 3 times higher than
392 transpiration in the silty soil. For the same soil, transpiration per unit root length of the irrigated treatment
393 was slightly larger than in the rainfed plot.

394 The differences in sap flow per plant between water treatments and soil types were more pronounced in
395 2018 (Supplementary material S9). The highest transpiration rate was observed in the irrigated plots (F1P3

396 & F2P3), followed by the rainfed plot of the silty soil (F2P2) and it was lowest in the rainfed plot of the
397 stony soil (F1P2). These observations were in line with the differences in biomass and leaf area index
398 between the treatments (Supplementary material 3b & 3d) and plant size (Supplementary material 6b-c-
399 d). In 2018, severe leaf rolling was observed in the rainfed plot (F1P2) from the beginning of June until the
400 end of the growing period in 2018 (Supplementary material 3d). Similar to 2017, transpiration per unit of
401 root length was much higher in the stony plots as compared to silty plots. Also, for the silty soil,
402 transpiration per unit of root length of the irrigated plot (F2P3) was higher than in the rainfed plot (F2P2).
403 Higher cumulative transpiration in the irrigated plots did not result in higher transpiration use efficiency
404 (TUE) in both soil types (Figure 10). For instance, TUE were 16.87 g mm^{-1} and 15.59 g mm^{-1} for F1P2 and
405 F2P2, respectively, while they were 15.47 and 14.79 g mm^{-1} for F1P3 and F2P3, respectively, in 2017 (Figure
406 10A). For the same soil, the rainfed plot showed slightly higher TUE than the irrigated plot. When
407 comparing the TUE of maize of the two soil types for the same water treatment, TUE at the stony soil was
408 almost the same in silty soil. The TUE was not much different among treatments and soil types in 2018.
409 Overall, TUE in 2017 was higher as compared to 2018 (Fig. 10b).

410 [Insert Figure 10 here]

411 **4. Discussions**

412 **4.1. Effects of soil types, water application, and climatic condition on root growth**

413 Our root observations showed that soil type considerably affected root growth more than water treatment
414 (Figure 2). Root growth was strongly inhibited by the stony soil where much lower root length was
415 observed than in the silty soil, especially in the deeper soil layers. This was consistent with the findings
416 reported in (Morandage et al., 2021) where a linear increase of stone content resulted in a linear decrease
417 of rooting depth across all stone contents and developmental stages. Also, both simulations and
418 observations indicated that rooting depth was increased due to the presence of cracks in the lower

419 minirhizontron facility (Morandage et al., 2021) which could explain the high root length between 40 and
420 120 cm soil depths which was observed in the silty soil in both years.

421 Jorda et al., (2022) reported a wide range of ratios of root length to shoot biomass from 200 to 1000 cm
422 g^{-1} around flowering time of maize depending on the wild type and root hair mutant genotypes growing
423 on either loamy or sandy soils. More roots and higher ratios of root length to shoot biomass were found
424 in the sand than in the loam in both wild type and root hair mutant genotypes (Jorda et al., 2022; Vetterlein
425 et al., 2022). Cai et al., (2018) observed much larger ratios of root length to shoot biomass in drought
426 stressed plots than in irrigated plot in both soil types in winter wheat which indicated the alternation of
427 sink: source relationships to cope with water stress. This study emphasized that more assimilates are used
428 to promote root growth and extract more water under drought stress. However, this was not the case for
429 the stony soil in our work where the drought stress was more pronounced, especially in 2018. A drop of
430 soil water potential (Supplementary material 2b), thus effective soil water potential (Figure 6a) was
431 substantial from 10th July 2018 toward the harvest in the rainfed plot in the silty soil (F2P2) which was
432 consistent with the reduction of leaf water potential (Fig. 6b), leaf area (Supplementary material 3c), total
433 dry matter (Supplementary material 3d), and crop height (Supplementary material 6b) as compared the
434 irrigated plot (F2P3). This indicates a mild water stress in 2018 in the rainfed plots on the silty soil. The
435 larger ratios of root length to shoot biomass in this F2P2 plot in 2018 as compared to F2P3 could be
436 explained by the change of source: sink relations where more assimilates were devoted to root growth,
437 even at a later growth stage. Moreover, the low stone content and soil cracks (Morandage et al., 2021)
438 might favor root growth in the deeper soil layers which are close to the shallow soil water table in the
439 rhizotrone facility with silty soil (Vanderborght et al., 2010). In conclusion, both soil texture and water
440 conditions influenced the root growth, however, the effects of the former on root length was more
441 pronounced than the later.

442 **4.2. Effects of soil types, water application, and climatic condition on stomatal conductance,**
443 **photosynthesis, transpiration, leaf water potential, and plant hydraulic conductance**

444 **4.2.1. Leaf water potential and stomatal conductance as affected by soil water conditions**

445 In the previous work, Koehler et al., (2022) reported that maize stomata closed at lower negative leaf
446 water potentials in sand than in loam growing under controlled environment. Cai et al., (2022b)
447 investigated transpiration response of pot-grown maize in two contrasting soil textures (sand and loam)
448 and exposed to two consecutive VPD levels (1.8 and 2.8 kPa). Transpiration rate decreased at less negative
449 soil matric potential in sand than in loam at both VPD levels. In sand, high VPD generated a steeper drop
450 in stomatal conductance with decreasing leaf water potential which indicated that the transpiration and
451 stomatal responses depend on soil hydraulics. In our study, stomata closed earlier and at more negative
452 soil and leaf water potentials in the stony soil than in the silty soil (see Fig. 4 & 7 and Supplementary
453 material 4 & 5). The lower soil water holding capacity of the stony soil compared to the silty soil resulted
454 in lower soil water potential and smaller total plant hydraulic conductance which in turn led to earlier
455 stomatal closure and to more negative soil water potential in the stony soil.

456 Stomatal control is an early and effective response to water stress to prevent the plant from water loss
457 and dehydration. Maize is considered as an isohydric plant which closes its stomata to maintain leaf water
458 potential above critical levels (Tardieu and Simonneau, 1998). Our results showed that minimum leaf
459 water potential varied among treatments (-1.5 MPa for F1P3, F2P2, and F2P3 and up to -2 MPa for F1P2
460 in 2017, while in 2018 minimum values were -2 MPa for F2P3, F2P2, and F2P3 and -2.7 MPa for F1P2) (Fig.
461 5, Fig. 6, and Fig. 7). In conclusion, our results confirmed that the minimum ψ_{leaf} was influenced by soil
462 types, soil hydraulic conductance, and atmospheric demand.

463 **4.2.2. Hydraulic conductance components as affected by soil water conditions**

464 Estimates of hydraulic components in soil-plant-atmosphere continuum are important not only to
465 understand its underlying relationship to other crop characteristics (stomatal conductance, transpiration,
466 and photosynthesis) but also to provide modeling parameters in process-based soil-root-shoot models
467 (Nguyen et al., 2020; Sulis et al., 2019; Nguyen et al., 2022b). Measurement of the components of hydraulic
468 conductance are challenging under field conditions because it requires the estimation of transpiration and
469 root to leaf water potential gradients. To our knowledge, our results were unique with regard to the
470 dynamics of $K_{\text{soil_plant}}$ for field-grown maize on two soil types and under contrasting water, and climate
471 conditions. Our seasonal $K_{\text{soil_plant}}$ ranged from 0.12 mm h⁻¹ MPa⁻¹ to 0.9 mm h⁻¹ MPa⁻¹ (Fig. 6 & Fig. 7; Fig.
472 8, and Supplementary material 7). Root system hydraulic conductance ranged from 0.26 to 1.47 mm h⁻¹
473 MPa⁻¹ (Figure 9). Note that the unit of $K_{\text{soil_plant}}$ as mm h⁻¹ MPa⁻¹ could be equivalent to the unit of 10⁻⁵ h⁻¹
474 if one assumes 1MPa is approximately 10⁵ mm in terms of pressure head. Cai et al., (2018) reported root
475 hydraulic conductance in winter wheat from 0.05 to 0.5 mm h⁻¹ MPa⁻¹ in two similar soil types. Nguyen et
476 al., (2020) also reported $K_{\text{soil_plant}}$ in winter wheat from 0.0625 to 0.461 mm h⁻¹ MPa⁻¹. Meunier et al., (2018)
477 focused on estimating the root system hydraulic conductance of maize in a container experiment where
478 the range of $K_{\text{soil_plant}}$ was much larger from 0.37 to 36 mm h⁻¹ MPa⁻¹ for the plant density of 10 plant m⁻².
479 Jorda et al., (2022) estimated root system hydraulic conductance of 0.5 to 1.5 10⁻³ d⁻¹ which would be
480 roughly between 2 to 6 mm h⁻¹ MPa⁻¹. In our work, except the F2P2 in 2018, the stem hydraulic
481 conductance was 10% to 60% higher than root system hydraulic conductance. This is in line with the report
482 from Gallardo et al., (1996) that stem hydraulic conductance of lupin was two times higher than root
483 system conductance regardless of measured days. This emphasizes the values of stem hydraulic
484 conductance compared to the root hydraulic conductance in maintaining water potential gradient from
485 shaded leaf or plant color to the sunlit leaf.

486 Our results showed clear differences in $K_{\text{soil_plant}}$ among treatments where much lower $K_{\text{soil_plant}}$ was
487 observed in the F1P2 as compared to F2P2 (see Figure 8 for 2018; Figure 6 and 7 and Supplementary

488 material 7 for both years). This indicated the soil texture dependence for whole plant hydraulic
489 conductance. Maize plants with the shorter root system (i.e. rainfed plot in the stony soil in 2018) (Fig. 3)
490 had lower plant hydraulic conductance. Our results indicated that there was an impact of soil hydraulic
491 conditions on $K_{\text{soil_plant}}$ via the reduction of root system hydraulic conductance. Our analysis for three
492 consecutive measurement days in 2018 (Fig 8) showed that in the silty soil, $K_{\text{soil_plant}}$ decreased when soil
493 water potentials are becoming more negative. For instance, in the silty soil in 2018 when the soil water
494 potentials were considerably lower in the rainfed than in the irrigated plot (e.g. after 10th July), $K_{\text{soil_plant}}$
495 was lower in the rainfed than in the irrigated plot. In the stony soil, the $K_{\text{soil_plant}}$ and leaf water potentials
496 seems to decrease more considerably (compared to the silty soil) when the soil water potentials become
497 more negative. In other words, $K_{\text{soil_plant}}$ increased considerably when the soil water potentials in the stony
498 soil increased. In our work, $K_{\text{soil_plant}}$ increased slowly after irrigation mainly for the severe water stress plot
499 (see F1P2 on 19 July in Fig 7d and 8c). This implied that added soil water by irrigation took some time for
500 recovery the soil-root contact within the rhizosphere.

501 **4.2.3. Relationships of stomatal conductance, transpiration, photosynthesis with plant hydraulic** 502 **variables**

503 The transpiration rate and $K_{\text{soil_plant}}$ (slope of linear regression lines in Fig. 8a and b) were very low in the
504 rainfed plot under the stony soil (F1P2) which was associated with the large $\psi_{\text{difference}}$ (Fig. 8a & b) and the
505 lower stomatal conductance as compared to other plots (Fig. 7c). The $K_{\text{soil_plant}}$ slightly increased after
506 irrigation (18 July - DOY 199 in Fig. 8b) corresponding with the smaller $\psi_{\text{difference}}$ (Fig. 8b) and an increase in
507 stomatal conductance (Fig. 7c). Seasonal $K_{\text{soil_plant}}$ was low in the rainfed plot under stony soil (F1P2) with
508 the larger $\psi_{\text{difference}}$ (Supplementary material 7). In addition, our study showed that the midday stomatal
509 conductance, photosynthesis, and transpiration were significantly correlated only with midday $K_{\text{soil_plant}}$ in
510 the rainfed plot on the stony soil (F1P2) in 2018 where high VPD and temperature occurred
511 (Supplementary material 10, 11, and 12). Maize plants had lower plant hydraulic conductance and more

512 negative soil water potential in the rainfed plot in stony soil that and they exhibited earlier stomatal
513 closure as compared to the same plot in the silty soil. This was in line with a study from Abdalla et al.,
514 (2022) which suggested that during soil drying, stomatal regulation of tomato is controlled by root and soil
515 hydraulic conductance. Recent work from Müllers et al., (2022) on faba bean and maize suggested that
516 differences in the stomatal sensitivity among plant species can be partly explained by the sensitivity of
517 soil-plant hydraulic conductance to soil drying. The loss of conductance has immediate consequences for
518 leaf water potential and the associated stomatal regulation. Cai et al., (2022b) also showed that the
519 decrease in sunlit leaf stomatal conductance was well correlated with the drop in soil-plant hydraulic
520 conductance, which was significantly affected by soil texture. This was confirmed in our work where the
521 stony soil strongly impacted on root growth, modulated $K_{\text{soil_plant}}$, and consequently influenced the leaf
522 stomatal conductance, photosynthesis, and transpiration.

523 **4.3. Relative contribution of water control by leaves and roots on transpiration and transpiration use** 524 **efficiency**

525 Responses of crops via stomatal control to reduce water loss at leaf scale while maintaining leaf
526 photosynthesis and water use efficiency were reported earlier (Nguyen et al., 2022a; Vitale et al., 2007).
527 In our study, leaf rolling was observed in both rainfed plots on the stony and the silty soil in the second
528 week of June 2017 and from the beginning of June until the end of the growing period in 2018. This
529 indicates another dehydration avoidance mechanism resulting from morphological adjustments which is
530 an effective mechanism for delaying senescence (Aparicio-Tejo and Boyer, 1983; Richards et al., 2002).
531 Stomatal closure resulted in more reduction of transpiration and assimilation in the rainfed plots than
532 irrigated plots with the same soil type (Fig. 4, Supplementary material 4 & 5, Fig. 5, and Supplementary
533 material 9a). There was reduction of shoot biomass (also stem size and leaf size adjustments) in F1P2 as
534 compared to other plots. However, the TUE was not smaller in this plot than the remaining plots. These

535 observations confirm that plant size adjustments through reduction of height, leaf width and length are
536 efficient responses to reduce water loss at canopy scale in addition to stomatal control at the leaf level.

537 Relative contribution of leaf area to transpiration has been highlighted in wheat where reduction of tiller
538 number resulted in significantly lower LAI, thus lower canopy transpiration (Cai et al., 2018; Trillo and
539 Fernández, 2005; Nguyen et al., 2022a). However, root system conductance per unit of leaf area and per
540 unit root mass were strongly reduced and eventually more than reduction of leaf area under water stress
541 (Trillo and Fernández, 2005). In our work, expressing the transpiration per unit of root length on the one
542 hand allowed to analyze the role of total root length to water uptake. However, on the other hand, the
543 lower total root length did not necessarily result in a lower root water uptake and vice versa. For instance,
544 the rainfed plot of the treatment F2P2 had the larger total root length which could postpone the effect of
545 soil water limitations in drying soils due to greater ability to extract water from subsoils. Therefore,
546 transpiration was very similar between F2P2 and F2P3. Despite of the much lower total root length in the
547 stony soil, $K_{\text{soil_plant}}$ in the irrigated plot (F1P3) was not much lower than in the same water treatment in
548 the silty soil (F2P3, Fig. 6d, 7d, Fig. 8, and Supplementary material 7). This could be explained by the fact
549 that the $K_{\text{soil_plant}}$ variability was not only depended on root architecture (here the root length and
550 distribution) but also depended on the variability of root segment hydraulic properties which has also been
551 illustrated and discussed in Zwieniecki et al. (2002), Frensch and Steudle (1989), Meunier et al. (2018),
552 Couvreur et al. (2014), and Ahmed et al. (2018). Moreover, the contribution of shoot hydraulic
553 conductance could be large in plants (Gallardo et al., 1996; Trillo and Fernández, 2005; Sunita et al., 2014)
554 which also confirmed in our work. In our work, $K_{\text{soil_plant}}$ comprised root and shoot conductance which are
555 directly influenced by soil hydraulics. Our estimates of $K_{\text{soil_plant}}$ varied with transpiration and gradients of
556 $\psi_{\text{sunlitleaf}}$ and $\psi_{\text{soil_effec}}$. Thus, any change of soil hydraulic conductance will change the root to shoot water
557 potential. Consequently, it will affect the gradients between shoot and root rhizosphere (Carminati and
558 Javaux, 2020). Thus, our study illustrates the importance of both soil texture characteristics and root

559 phenotypic traits (here root length) in regulating plant transpiration (Cai et al., 2022a). Other traits like
560 root hair density (Cai et al., 2022a) or higher root length density (Vadez, 2014) could contribute to the soil
561 to root water potential and root-zone hydraulic conductance where dense root hairs delayed soil water
562 deficit in drying soils. However, contrasting results have shown that root hairs did not have an effect on
563 root water uptake (see Jorda et al. 2022). The role of root hairs could not be analyzed in our work which
564 was based on the root data from minirhizotron images.

565 **5. Conclusion**

566 We presented plant hydraulic characteristics and crop growth from root to shoot of maize under field-
567 grown conditions with two soil types (silty and stony), each soil with two water regimes (irrigated and
568 rainfed) for two growing seasons (2017, 2018). Our results confirmed that root length and ratios of root
569 length to shoot biomass were modulated by soil types and water treatment but less by seasonal
570 evaporative demand. Increase ratio of root length to shoot biomass has been an important response of
571 maize that allows plants to extract more water under drought stress that occurred rather in the silty soil
572 but less in the stony soil due to the higher content of stony material. Despite of lower root length in the
573 stony irrigated plot, transpiration rate was not much lower than in the silty irrigated plot. This could be
574 related to another property of the root such as root segment conductance or other root traits (e.g. root
575 hair). Further investigation with extensive measurements of roots including axial and radial root
576 conductance at field scale will be required to better explain the observed results.

577 Another conclusion is that stomatal regulation maintains leaf water potential at certain thresholds which
578 depends on soil types, soil water availability, and seasonal atmospheric demand. The stomata conductance
579 was smaller and decreased at more negative leaf water potentials in stony soil than in silty soil. The leaf
580 water potentials are affected by the soil-plant hydraulic conductance. In addition to stomatal regulation,
581 leaf growth and plant size adjustments are important to regulate the transpiration and water use efficiency
582 in the same year.

583 The lowest soil-plant hydraulic conductance was observed in the stony soil with severe drought stress as
584 compared to silty soil while its variation depends also on the soil water variation (before and after
585 irrigation). Root system and soil-plant hydraulic conductance depended strongly on soil hydraulic
586 properties. In the stony soil, which has a considerably smaller water holding capacity than the silty soil,
587 root length was considerably smaller than in the silty soil. Nevertheless water uptake per unit root length
588 was much larger than in the fine soil. This also means that the hydraulic conductance per unit root length
589 must have been much larger in the stony soil than in the fine soil. Cai et al., (2018) observed a similar effect
590 for winter wheat but they found much smaller differences in the root length normalized root conductance.
591 The higher root length normalized root conductance means that the anatomy of the root tissues must
592 have been influenced by the soil texture and compensated the considerably smaller root length in the
593 stony soil. Looking at the effect of water treatments in the silt soil, the non-irrigated plot had more roots
594 than the irrigated one and both had more roots in the year with high VPD. But the soil-root conductance
595 was higher in the irrigated plot than in the rainfed plot. This means that in the irrigated plot, the soil-root
596 conductance per unit root length was higher than in the rainfed plot. This could either be due to wetter
597 soil conditions and higher soil conductance or it could be due to a larger conductance of the root tissues.
598 Especially in 2017 when the silty soil was wetter, the slightly larger soil-root conductance in the irrigated
599 plot is most likely the result of larger root tissue conductance in the irrigated plot. Thus, how root
600 architecture (here represented simply by the total root length) and root tissue conductivities 'respond' to
601 drought stress might be opposite depending on the comparisons that are made. When the stony soil and
602 silt soil are compared, the higher 'stress' due to lower water availability in the stony soil resulted in less
603 roots with a higher root tissue conductance in the soil with more stress. When comparing the rainfed with
604 the irrigated plot in the silty soil, the higher stress in the rainfed soil resulted in more roots with a lower
605 root tissue conductance in the treatment with more stress. This illustrates that the 'response' to stress can
606 be completely opposite depending on conditions or treatments that lead to the differences in stress that
607 are compared. Therefore, it cannot be the 'stress' alone that defines how a plant will react and adapt its

608 root system. Modelling the impact of stress and the feedback between drought stress and plant
609 development is likely controlled by other properties or parameters that change with changing soil water
610 availability and atmospheric water demand than the plant stress level. Results from this study show that
611 soil-crop models should focus not only on simulating stomatal regulations to capture the response to
612 drought stress, but also require adequate representations of leaf growth and adjustments.

613 **Acknowledgements**

614 This work has partially been funded by Federal Ministry of Education and Research (BMBF) through
615 European SUSCAP project – 031B0170B and COINS project and the Deutsche Forschungsgemeinschaft
616 (DFG, German Research Foundation) under Germany’s Excellence Strategy – EXC 2070 – 390732324”. We
617 acknowledge the support by the SFB/TR32 “Pattern in Soil–Vegetation–Atmosphere Systems: Monitoring,
618 Modelling, and Data Assimilation” funded by the Deutsche Forschungsgemeinschaft (DFG). Thuy Nguyen
619 and Thomas Gaiser also thank the DETECT – CRC 1502 research program which is funded by DFG. We thank
620 Dr. Matthias Langensiepen for his supports and technical help in the TR32 project. We would like to thank
621 all the student assistants and technicians for their considerable efforts to collect the data in the field and
622 the laboratories.

623

624

625

626

627

628

629

630 **List of Tables**

631 Table 1. Crop phenology and management information for different treatments in 2017 and 2018.

Soil types	2017				2018			
	Stony (F1)	Stony (F1)	Silty (F2)	Silty (F2)	Stony (F1)	Stony (F1)	Silty (F2)	Silty (F2)
Water treatments	Rainfed (P2)	Irrigated (P3)	Rainfed (P2)	Irrigated (P3)	Rainfed (P2)	Irrigated (P3)	Rainfed (P2)	Irrigated (P3)
Plot names	F1P2	F1P3	F2P2	F2P3	F1P2	F1P3	F2P2	F2P3
Growing season (days) [‡]	136	136	136	136	107	107	107	107
Cumulative rainfall (mm) [*]	248.7	248.7	248.7	248.7	91.3	91.3	91.3	91.3
Irrigation (mm)	0	130	0	130	66	257.6	0	257.6
Fertilizer application (mm/dd) (per hectare)	05/09:100 kg N + 40kg P ₂ O ₅ 07/06: 80 kg N + 40 kg K ₂ O				05/22: 100 kg N 05/30: 40 kg P ₂ O ₅ + 40 kg K ₂ O 06/27: 80 kg N			
Sowing date (mm/dd)	05/04				05/08			
Emergence date	05/09				05/13			
Tasseling date	07/09				07/09			
Silking date	07/14				07/11			
Harvest date	09/12				08/22			

632 Notes: [‡] from sowing to harvest; ^{*} for rainfall for whole growing season;

List of Figures

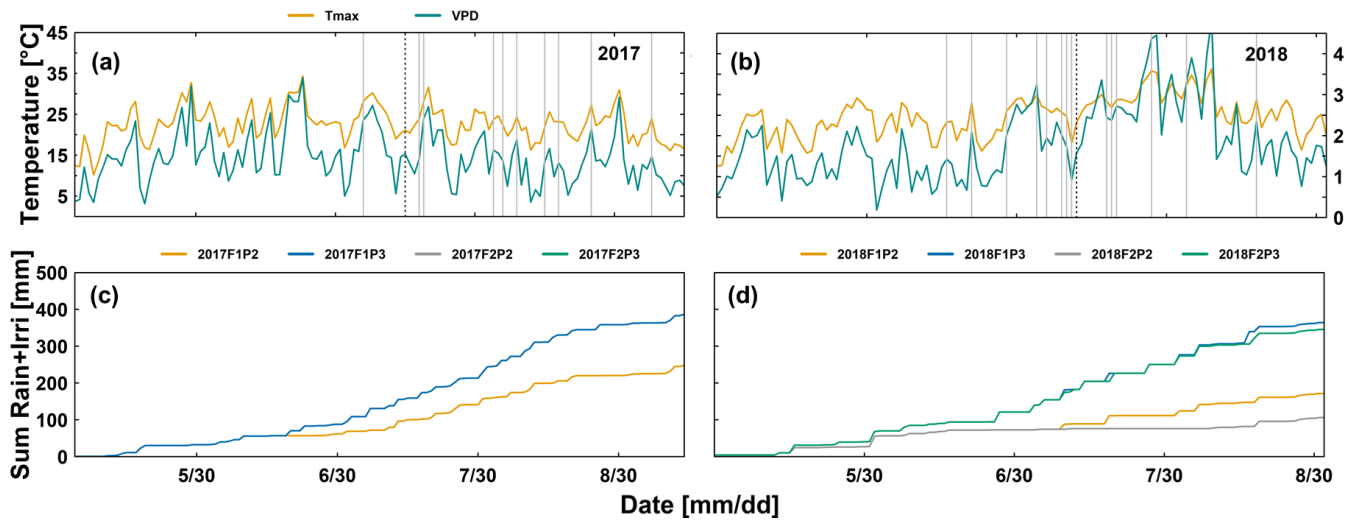


Figure 1: Daily maximum air temperature (Tmax) (°C), daily maximum air vapor pressure deficit (VPD) (kPa) in the two growing seasons (a) 2017 and (b) 2018 and cumulative (sum) of rainfall and irrigation from the rainfed (P2) and irrigated (P3) plots of the stony soil (F1) and silty soil (F2) in the two growing seasons (c) 2017 and (d) 2018. The black dashed vertical lines (a) and (b) indicate silking time. Grey vertical lines in (a) and (b) indicate the measured days for leaf gas exchange and leaf water potential. Two lines for 2017F2P2 and 2017F2P3 were overlapped by the lines from 2017F1P2 and 2017F1P3, respectively

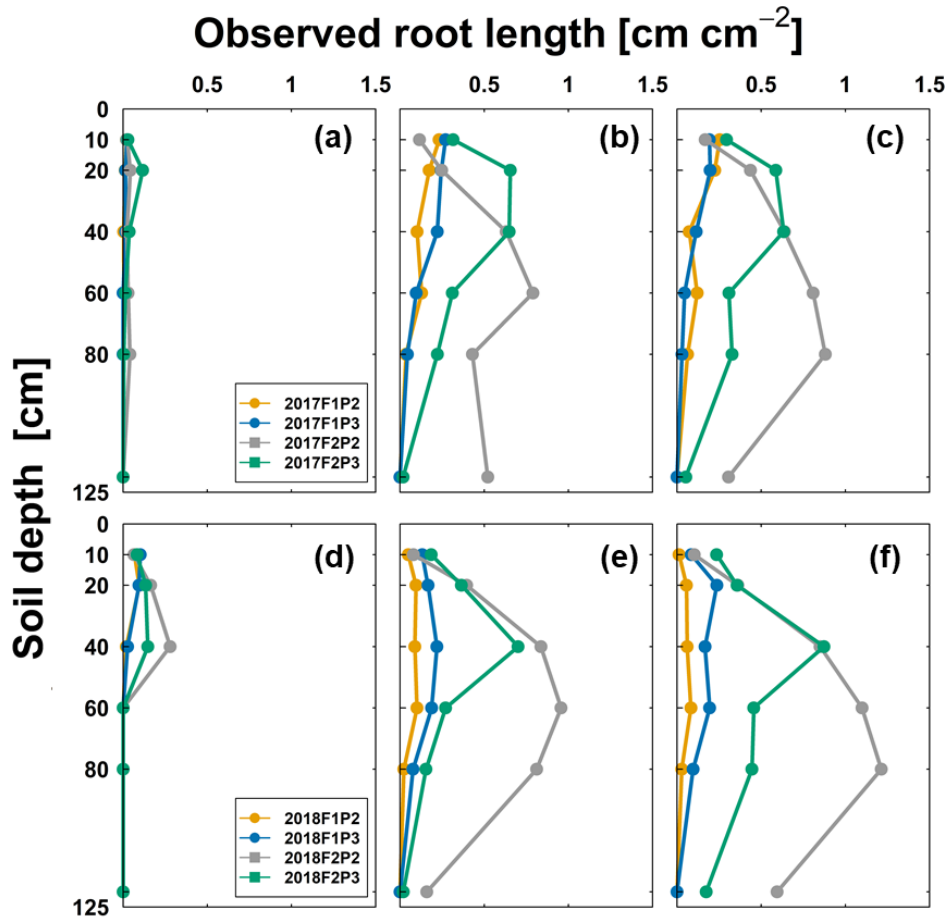


Figure 2: Observed root length from minirhizotubes (cm cm^{-2}) from 10, 20, 40, 60, 80, and 120 cm soil depth from the rainfed (P2) and irrigated (P3) plots of the stony soil (F1) and silty soil (F2) in the two growing seasons in 2017 (a - 8 June, b - at silking on 13 July, c - at harvest on 12 September) and in 2018 (d - 7 June, e - at one week after silking - 18 July, f - one week before harvest - 16 August).

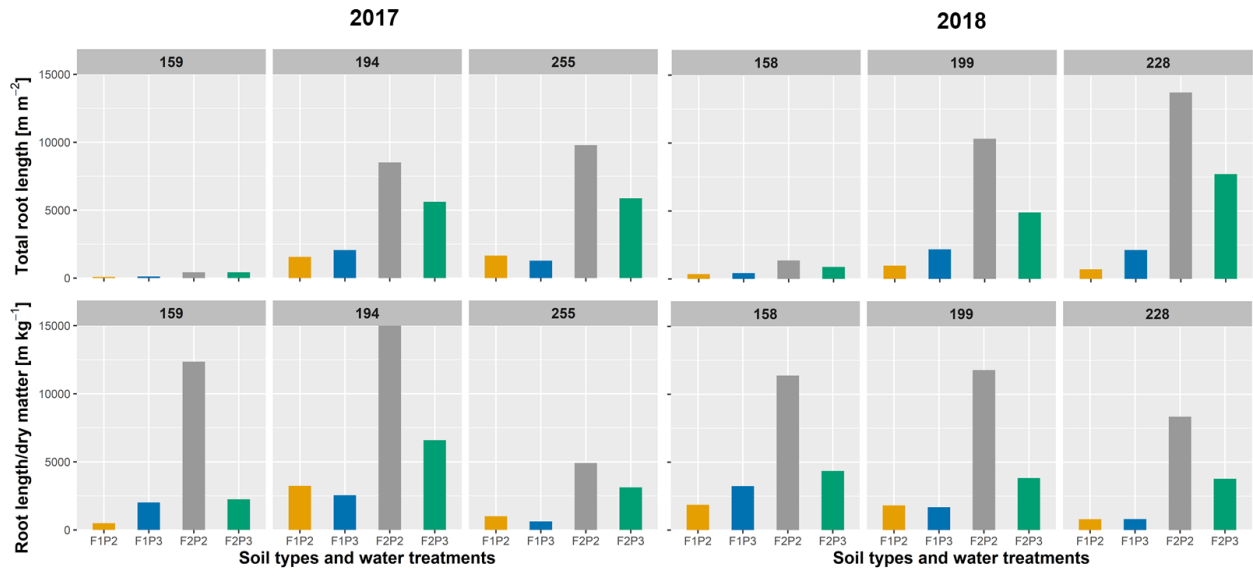


Figure 3: Observed root length from minirhizotubes (m m^{-2}) and ratio of root length per shoot dry matter (m kg^{-1}) from the rainfed (P2) and irrigated (P3) plots of the stony soil (F1) and silty soil (F2) in the two growing seasons (DOY 159, 194, and 255, left panel) in 2017 and in 2018 (DOY 158, 199, and 228, right panel) where on 8 June (DOY 159) at silking on 13 July (DOY194) 2017; and at harvest on 12 September (DOY 255) in 2017; 7 June (DOY 158), one week after silking on 18 July (DOY 199); and one week before harvest on 16 August (DOY 228) in 2018 (see also Figure 2).

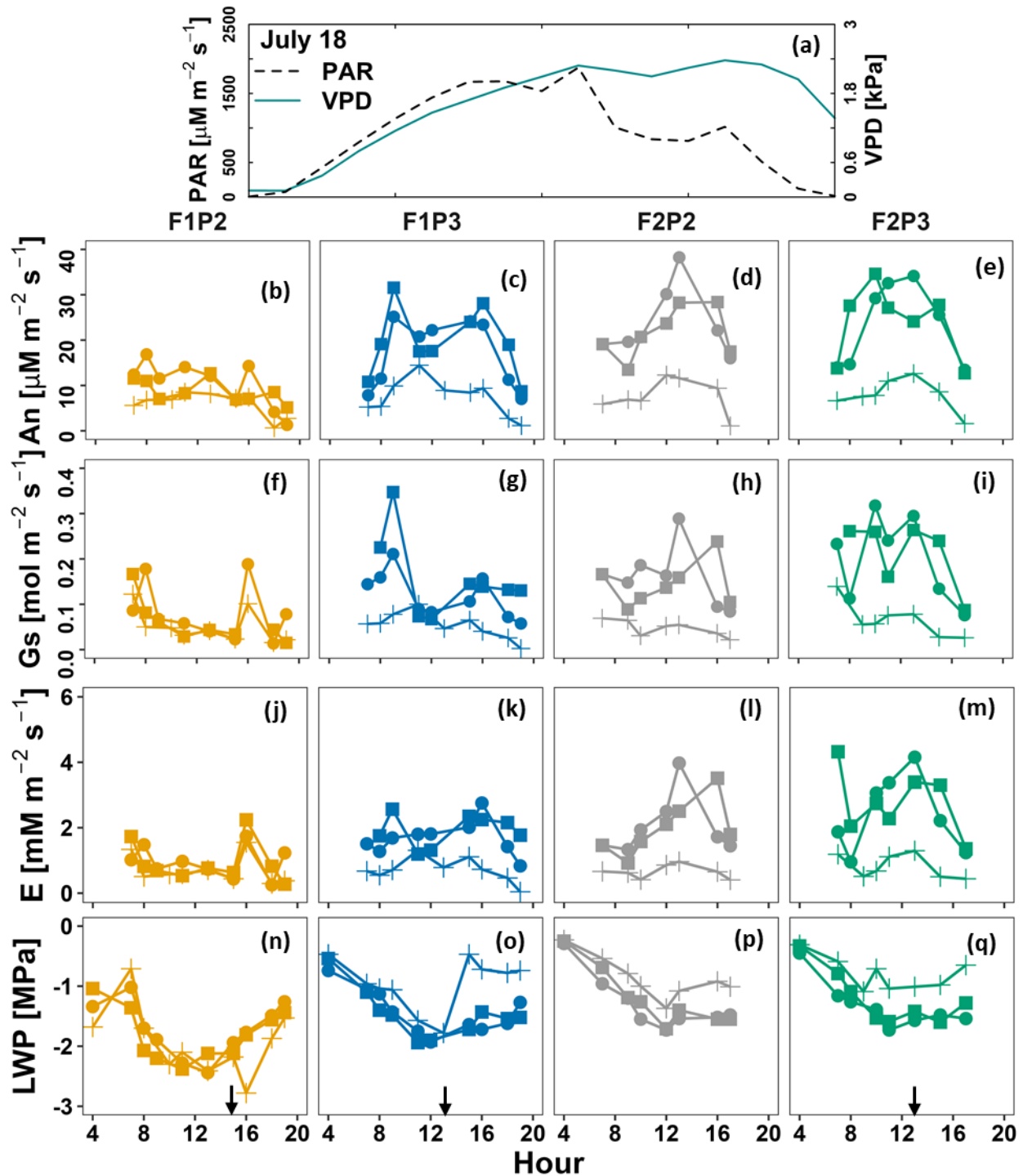


Figure 4. Diurnal course of (a) photosynthetically active radiation (PAR) and vapor pressure deficit (VPD), (b–e) leaf net photosynthesis (An), (f–i) leaf stomatal conductance (Gs), (j–m) leaf transpiration (E), and (n–q) leaf water potential (LWP) on 18 July in maize in 2018 before irrigation at the rainfed (P2) and irrigated (P3) plots of the stony soil (F1) and silty soil (F2). Measurement was carried out from shaded leaf (plus symbol with line) and two sunlit leaves (solid dot - lines and solid square - lines). Crop was irrigated at 1 PM, 1 PM, 4 PM for F1P3, F2P3, and F1P2, respectively (22.75 mm for each plot) (Supp. 2). Black arrows indicate time of irrigation.

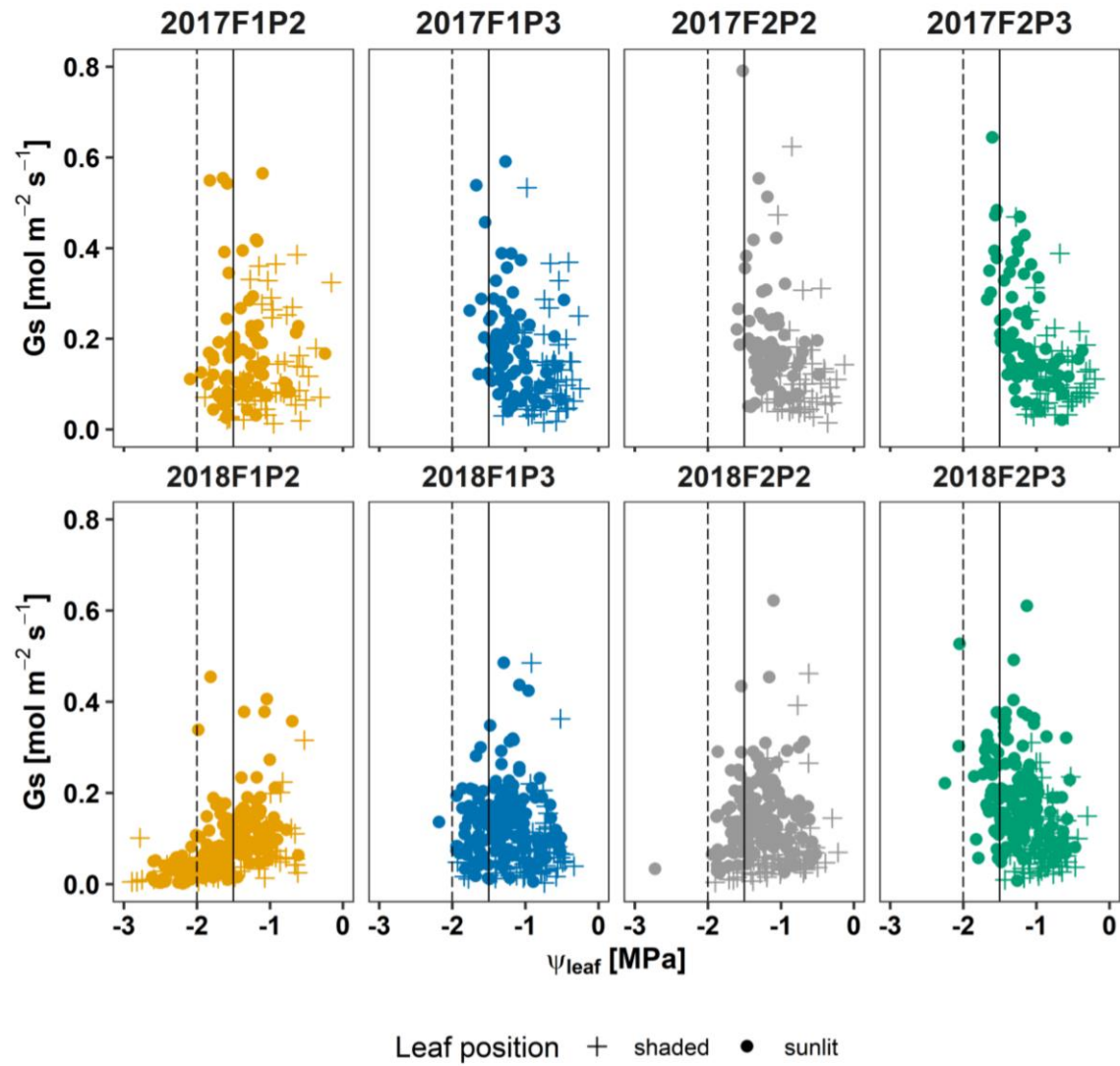


Figure 5: Seasonal stomatal conductance to water vapor (G_s) versus leaf water potential (ψ_{leaf}) in 2017 (top panel) and in 2018 (bottom panel) at the rainfed (P2) and irrigated (P3) plots of the stony soil (F1) and silty soil (F2). Vertically continuous and dashed lines indicated ψ_{leaf} at -1.5 and -2 MPa, respectively. Measurement was carried out from shaded leaf (plus symbol) and two sunlit leaves (solid dots)

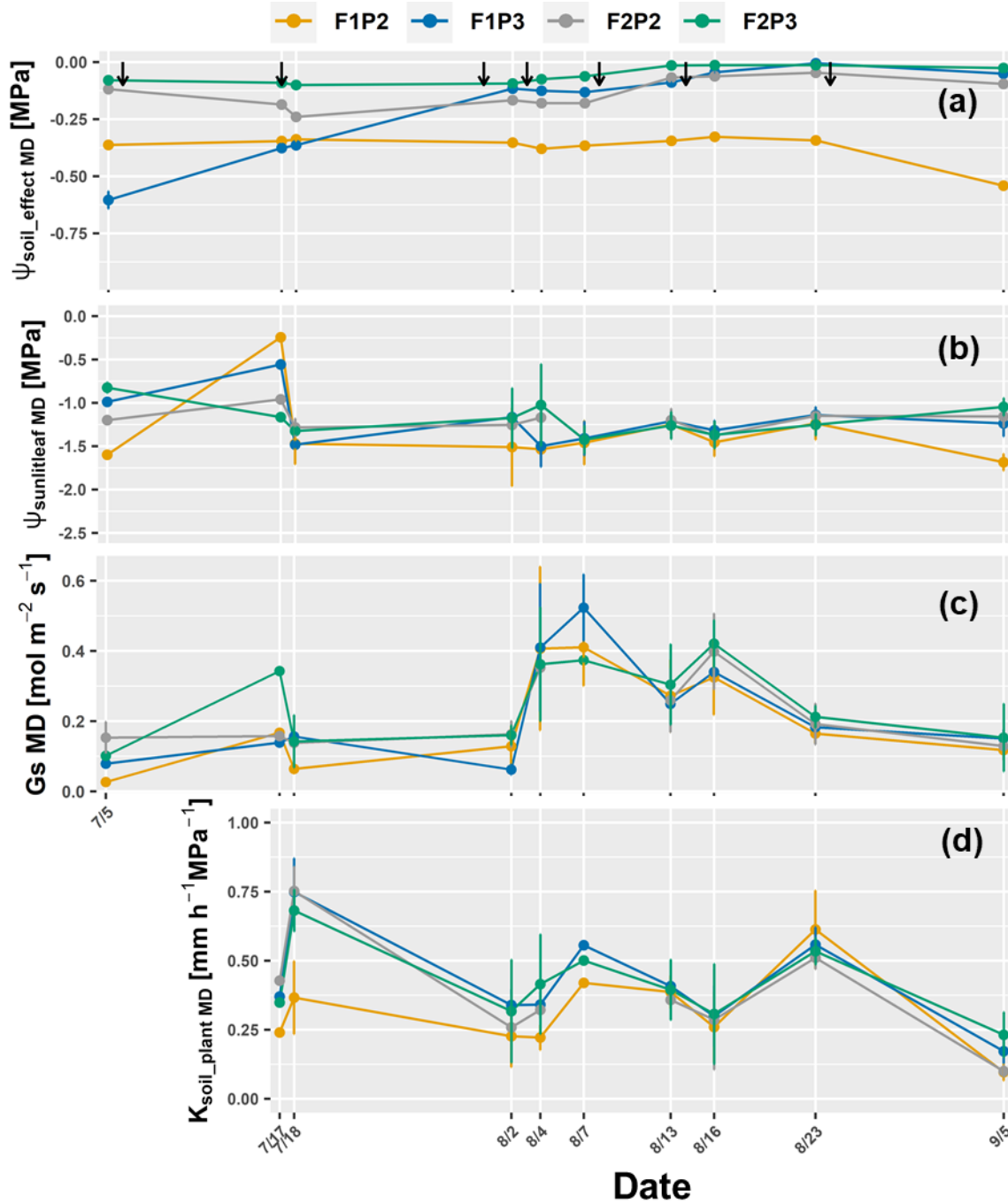


Figure 6: Dynamic of around midday (MD) of (a) the effective soil water potential ($\psi_{\text{soil_effec, MD}}$) (b) sunlit leaf water potential ($\psi_{\text{sunlitleaf MD}}$), (c) stomatal conductance (Gs MD) and (d) whole soil-plant hydraulic conductance ($K_{\text{soil_plant MD}}$) in the growing season 2017 from the rainfed (P2) and irrigated (P3) plots of the stony soil (F1) and silty soil (F2). Error bars indicate the standard deviation of the different values taken around midday (11 AM, 12AM, 1PM, and 2 PM) of different sunlit leaves. Whole soil-plant hydraulic conductance was shown from 17 July when sap flow was measured. The black arrows indicates the irrigation events for the irrigated treatments F1P3 and F2P3 in the showing period.

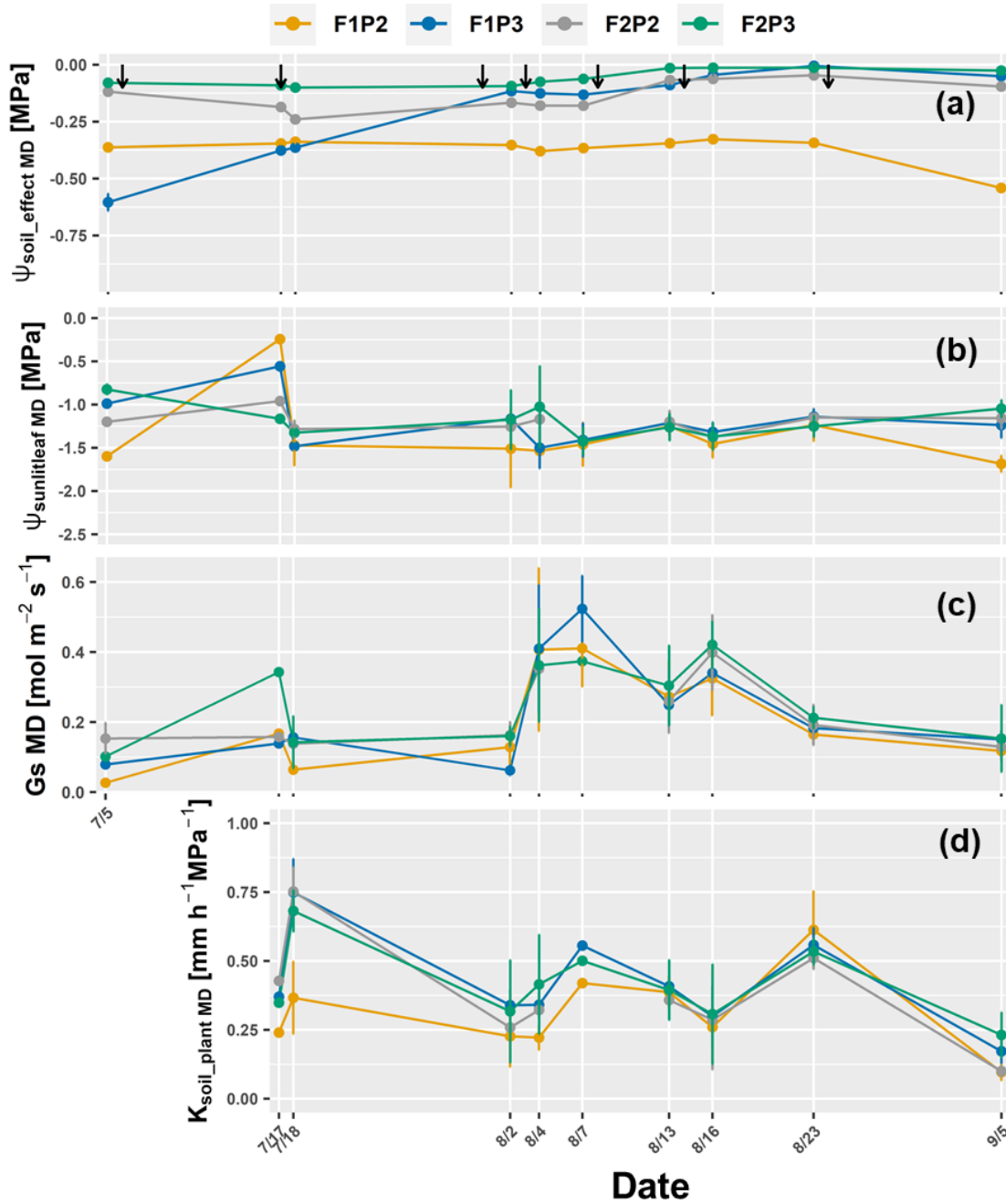


Figure 7: Dynamic of around midday (MD) of (a) the effective soil water potential ($\psi_{\text{soil_effec MD}}$) (b) sunlit leaf water potential ($\psi_{\text{sunlitleaf MD}}$), (c) stomatal conductance (Gs MD) and (d) whole soil-plant hydraulic conductance ($K_{\text{soil_plant MD}}$) in the growing season 2018 from the rainfed (P2) and irrigated (P3) plots of the stony soil (F1) and silty soil (F2). Error bars indicate the standard deviation of the different values taken around midday (11 AM, 12AM, 1PM, and 2 PM) Leaf water potential and stomatal conductance were 2 sunlit leaves and one shaded leaf at each measured hour. Whole soil-plant hydraulic conductance was shown from 3 July when sap flow was measured. The black arrows indicates the irrigation events for the irrigated treatments F1P3 and F2P3 while the orange arrow indicates the irrigation application for the rainfed plot at the stony soil (F1P2).

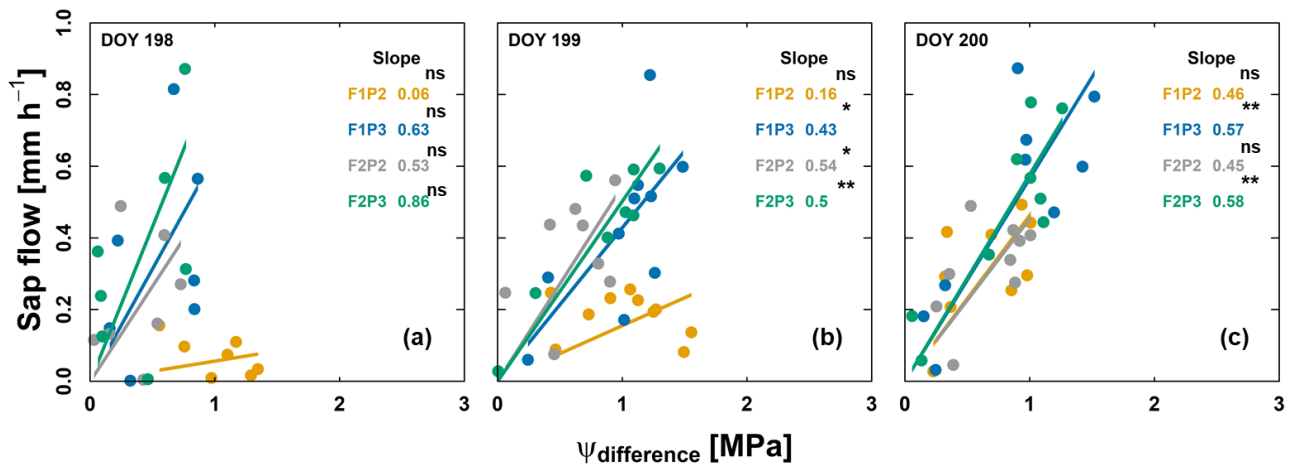


Figure 8: Relationship of sap flow and difference of effective soil water potential and sunlit leaf water potential ($\Psi_{\text{difference}}$) from the rainfed (P2) and irrigated (P3) plots of the stony soil (F1) and silty soil (F2) on three consecutive measurement days from predawn in 2018 (a) 17 July - DOY 198, (b) 18 July - DOY 199 and (c) 19 July - DOY 200. Crop was irrigated on 18 July (DOY 199) at 1 PM, 1 PM, and 4 PM for F1P3, F2P3, and F1P2, respectively (22.75 mm for each plot). The unit of slope in the linear regression (or soil-plant hydraulic conductance) is $\text{mm h}^{-1} \text{MPa}^{-1}$. Regression was based on the DEMING approach. The asterisk which are next to the slopes indicate a significant correlation between two variables according to Pearson method (ns: non-significant; * $p < 0.05$; ** $p < 0.01$; *** $p < 0.001$).

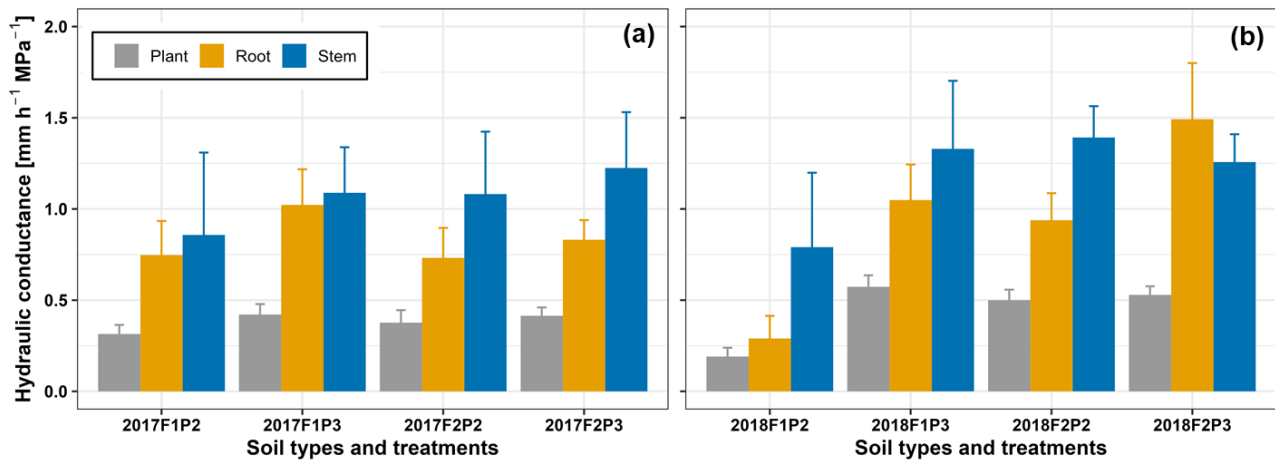


Figure 9: Comparison of different midday hydraulic components ($\text{mm h}^{-1} \text{MPa}^{-1}$): soil-plant (grey bars), soil-root (yellow bars), and stem (blue bars) from the rainfed (P2) and irrigated (P3) plots of the stony soil (F1) and silty soil (F2) in the two growing seasons (a) in 2017 and (b) in 2018. The error bars indicate the standard deviation from measurements around midday (11 AM, 12AM, 1PM, and 2 PM) in different measured days (in 2017 with $n = 4 \times 9$ days, Supplementary material 10, 11, and Fig. 6 and in 2018 with $n = 4 \times 10$ days, Supplementary material 10, 12, and Fig. 7).

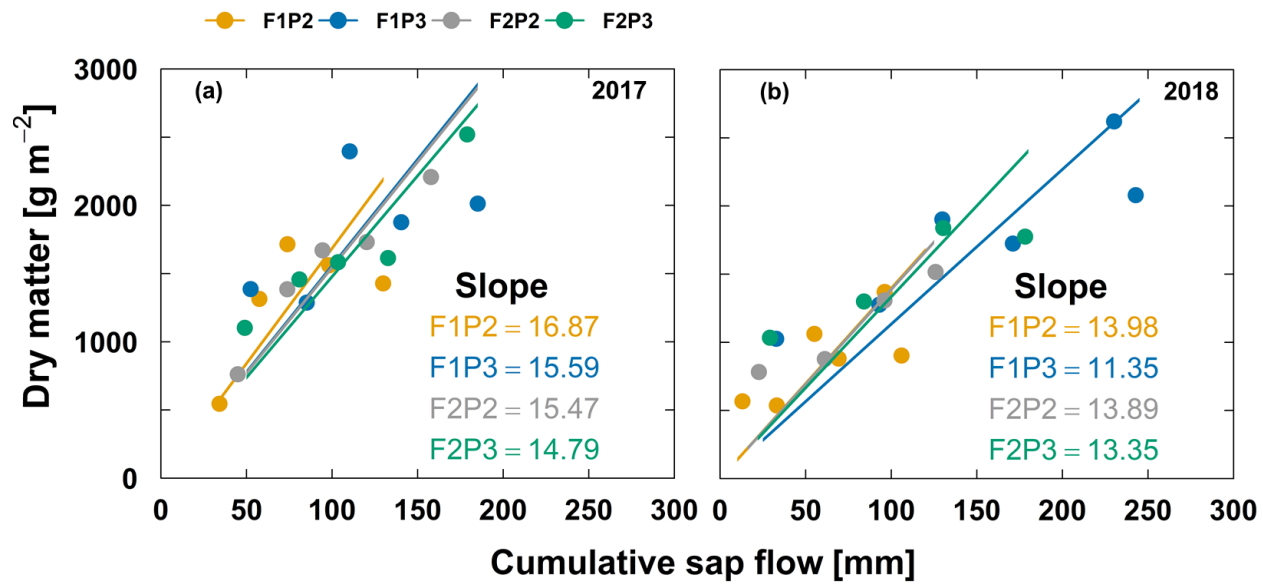


Figure 10: Relationship of aboveground dry matter and cumulative sap flow from the rainfed (P2) and irrigated (P3) plots of the stony soil (F1) and silty soil (F2) in the two growing seasons (a) 2017 and (b) 2018. The unit of slope linear relationship is g mm^{-1} . The less number of data points in (b) in 2018 from the F2P2 and F2P3 plots were due to the missing values of measured sap flow because of sensor disconnection. For aboveground dry matter, each point represents the average of two sampling replicates, except the harvest with 5 sampling replicates.

Reference

- Abdalla, M., M.A. Ahmed, G. Cai, F. Wankmüller, N. Schwartz, et al. 2022. Stomatal closure during water deficit is controlled by below-ground hydraulics. *Ann. Bot.* 129(2): 161–170. doi: 10.1093/aob/mcab141.
- Abdalla, M., A. Carminati, G. Cai, M. Javaux, and M.A. Ahmed. 2021. Stomatal closure of tomato under drought is driven by an increase in soil-root hydraulic resistance. *Plant. Cell Environ.* 44(2): 425–431. doi: 10.1111/pce.13939.
- Ahmed, M.A., M. Zarebanadkouki, F. Meunier, M. Javaux, A. Kaestner, et al. 2018. Root type matters: Measurement of water uptake by seminal, crown, and lateral roots in maize. *J. Exp. Bot.* 69(5): 1199–1206. doi: 10.1093/jxb/erx439.
- Aparicio-Tejo, P., and J.S. Boyer. 1983. Significance of Accelerated Leaf Senescence at Low Water Potentials for Water Loss and Grain Yield in Maize1. *Crop Sci.* 23(6): crops1983.0011183X002300060040x. doi: <https://doi.org/10.2135/crops1983.0011183X002300060040x>.
- Bauer, F.M., L. Lärm, S. Morandage, G. Lobet, J. Vanderborght, et al. 2021. Combining deep learning and automated feature extraction to analyze minirhizotron images: development and validation of a new pipeline. *bioRxiv* (1): 2021.12.01.470811. <https://www.biorxiv.org/content/10.1101/2021.12.01.470811v1%0Ahttps://www.biorxiv.org/content/10.1101/2021.12.01.470811v1.abstract>.
- Bornemann*, L., M. Herbst, G. Welp, H. Vereecken, and W. Amelung. 2011. Rock Fragments Control Size and Saturation of Organic Carbon Pools in Agricultural Topsoil. *Soil Sci. Soc. Am. J.* 75(5): 1898. doi: 10.2136/sssaj2010.0454.
- Bourbia, I., C. Pritzkow, and T.J. Brodribb. 2021. Herb and conifer roots show similar high sensitivity to water deficit. *Plant Physiol.* 186(4): 1908–1918. doi: 10.1093/plphys/kiab207.
- Cai, G., M.A. Ahmed, M. Abdalla, and A. Carminati. 2022a. Root hydraulic phenotypes impacting water uptake in drying soils. *Plant Cell Environ.* 45(3): 650–663. doi: 10.1111/pce.14259.
- Cai, G., M. König, A. Carminati, M. Abdalla, M. Javaux, et al. 2022b. Transpiration response to soil drying and vapor pressure deficit is soil texture specific. *Plant Soil* (0123456789). doi: 10.1007/s11104-022-05818-2.
- Cai, G., J. Vanderborght, V. Couvreur, C.M. Mboh, and H. Vereecken. 2017a. Parameterization of Root Water Uptake Models Considering Dynamic Root Distributions and Water Uptake Compensation. *Vadose Zo. J.* 0(0): 0. doi: 10.2136/vzj2016.12.0125.
- Cai, G., J. Vanderborght, A. Klotzsche, J. van der Kruk, J. Neumann, et al. 2016. Construction of Minirhizotron Facilities for Investigating Root Zone Processes. *Vadose Zo. J.* 15(9): 0. doi: 10.2136/vzj2016.05.0043.
- Cai, G., J. Vanderborght, M. Langensiepen, A. Schnepf, H. Hüging, et al. 2018. Root growth, water uptake, and sap flow of winter wheat in response to different soil water conditions. *Hydrol. Earth Syst. Sci.* 22(4): 2449–2470. doi: 10.5194/hess-22-2449-2018.
- Cai, Q., Y. Zhang, Z. Sun, J. Zheng, W. Bai, et al. 2017b. Morphological plasticity of root growth under mild water stress increases water use efficiency without reducing yield in maize. *Biogeosciences* 14(16): 3851–3858. doi: 10.5194/bg-14-3851-2017.

- Carminati, A., and M. Javaux. 2020. Soil Rather Than Xylem Vulnerability Controls Stomatal Response to Drought. *Trends Plant Sci.* 25(9): 868–880. doi: 10.1016/j.tplants.2020.04.003.
- Carminati, A., M. Zarebanadkouki, E. Kroener, M.A. Ahmed, and M. Holz. 2016. Biophysical rhizosphere processes affecting root water uptake. *Ann. Bot.* 118(4): 561–571. doi: 10.1093/aob/mcw113.
- Choudhary, S., and T.R. Sinclair. 2014. Hydraulic conductance differences among sorghum genotypes to explain variation in restricted transpiration rates. *Funct. Plant Biol.* 41(3): 270–275. doi: 10.1071/FP13246.
- Cochard, H. 2002. Xylem embolism and drought-induced stomatal closure in maize. *Planta* 215(3): 466–471. doi: 10.1007/s00425-002-0766-9.
- Comas, L.H., S.R. Becker, V.M. V. Cruz, P.F. Byrne, and D.A. Dierig. 2013. Root traits contributing to plant productivity under drought. *Front. Plant Sci.* 4(NOV): 1–16. doi: 10.3389/fpls.2013.00442.
- Coupeledru, A., É. Lebon, A. Christophe, A. Doligez, L. Cabrera-Bosquet, et al. 2014. Genetic variation in a grapevine progeny (*Vitis vinifera* L. cvs GrenacheSyrah) reveals inconsistencies between maintenance of daytime leaf water potential and response of transpiration rate under drought. *J. Exp. Bot.* 65(21): 6205–6218. doi: 10.1093/jxb/eru228.
- Couvreur, V., J. Vanderborght, X. Draye, and M. Javaux. 2014. Dynamic aspects of soil water availability for isohydric plants: Focus on root hydraulic resistances. *water Resour. Res.* 50: 8891–8906. doi: 10.1002/2014WR015608.Received.
- Couvreur, V., J. Vanderborght, and M. Javaux. 2012. A simple three-dimensional macroscopic root water uptake model based on the hydraulic architecture approach. *Hydrol. Earth Syst. Sci.* 16: 2957–2971. doi: 10.5194/hess-16-2957-2012.
- Daryanto, S., L. Wang, and P. Jacinthe. 2016. Global Synthesis of Drought Effects on Maize and Wheat Production. *PLoS One* 11(5): 1–15. doi: 10.1371/journal.pone.0156362.
- Draye, X., Y. Kim, G. Lobet, and M. Javaux. 2010. Model-assisted integration of physiological and environmental constraints affecting the dynamic and spatial patterns of root water uptake from soils. *J. Exp. Bot.* 61(8): 2145–2155. doi: 10.1093/jxb/erq077.
- Domec, J., and D.M. Johnson. 2012. Does homeostasis or disturbance of homeostasis in minimum leaf water potential explain the isohydric versus anisohydric behavior of *Vitis vinifera* L. cultivars? *Tree* 32: 245–248. doi: 10.1093/treephys/tps013.
- Domec, J., and M.L. Pruyn. 2008. Bole girdling affects metabolic properties and root, trunk and branch hydraulics of young ponderosa pine trees. *Tree Physiol.* (28): 1493–1504.
- Dynamax. 2007. Dynagage Sap Flow Sensor User Manual. 1–107. Last access on March 5th 2015.
- Effendi, R., S.B. Priyanto, M. Aqil, and M. Azrai. 2019. Drought adaptation level of maize genotypes based on leaf rolling, temperature, relative moisture content, and grain yield parameters. *IOP Conf. Ser. Earth Environ. Sci.* 270(1). doi: 10.1088/1755-1315/270/1/012016.
- Fang, J., and Y. Su. 2019. Effects of Soils and Irrigation Volume on Maize Yield, Irrigation Water Productivity, and Nitrogen Uptake. *Sci. Rep.* 9(1): 1–11. doi: 10.1038/s41598-019-41447-z.
- Frensch, J., and E. Steudle. 1989. Axial and Radial Hydraulic Resistance to Roots of Maize (*Zea mays* L.). *Plant Physiol.* 91: 719–726.

- Gallardo, M., J. Eastham, P.J. Gregory, and N.C. Turner. 1996. A comparison of plant hydraulic conductances in wheat and lupins. *J. Exp. Bot.* 47(295): 233–239. doi: 10.1093/jxb/47.2.233.
- Hochberg, U., F.E. Rockwell, N.M. Holbrook, and H. Cochard. 2018. Iso/Anisohydry: A Plant–Environment Interaction Rather Than a Simple Hydraulic Trait. *Trends Plant Sci.* 23(2): 112–120. doi: 10.1016/j.tplants.2017.11.002.
- Hopmans, J.W., and K.L. Bristow. 2002. Current Capabilities and Future Needs of Root Water and Nutrient Uptake Modeling. In: Sparks, D.L.B.T.-A. in A., editor, *Advances in Agronomy*. Academic Press. p. 103–183
- Hubbard, R.M., M.G. Ryan, V. Stiller, and J.S. Sperry. 2001. Stomatal conductance and photosynthesis vary linearly with plant hydraulic conductance in ponderosa pine. *Plant, Cell Environ.* 24(1): 113–121. doi: 10.1046/j.1365-3040.2001.00660.x.
- IPCC. 2022. Impacts, Adaptation, and Vulnerability. Working Group II Contribution to the IPCC Sixth Assessment Report of the Intergovernmental Panel on Climate Change.
- Jorda, H., M.A. Ahmed, M. Javaux, A. Carminati, P. Duddek, et al. 2022. Field scale plant water relation of maize (*Zea mays*) under drought – impact of root hairs and soil texture. *Plant Soil* 478(1–2): 59–84. doi: 10.1007/s11104-022-05685-x.
- Klein, T. 2014. The variability of stomatal sensitivity to leaf water potential across tree species indicates a continuum between isohydric and anisohydric behaviours. *Funct. Ecol.*: 1313–1320. doi: 10.1111/1365-2435.12289.
- Koehler, T., D.S. Moser, Á. Botezatu, T. Murugesan, S. Kaliamoorthy, et al. 2022. Going underground: soil hydraulic properties impacting maize responsiveness to water deficit. *Plant Soil* 478(1–2): 43–58. doi: 10.1007/s11104-022-05656-2.
- Lärm, L., F.M. Bauer, N. Hermes, J. van der Kruk, H. Vereecken, et al. 2023. Multi-year belowground data of minirhizotron facilities in Selhausen. *Sci. Data* 10(1): 1–15. doi: 10.1038/s41597-023-02570-9.
- Li, X., T.R. Sinclair, and L. Bagherzadi. 2016. Hydraulic Conductivity Changes in Soybean Plant-Soil System with Decreasing Soil Volumetric Water Content. *J. Crop Improv.* 30(6): 713–723. doi: 10.1080/15427528.2016.1231729.
- Li, Y., J.S. Sperry, and M. Shao. 2009. Hydraulic conductance and vulnerability to cavitation in corn (*Zea mays* L.) hybrids of differing drought resistance. *Environ. Exp. Bot.* 66(2): 341–346. doi: 10.1016/j.envexpbot.2009.02.001.
- Marin, M., D.S. Feeney, L.K. Brown, M. Naveed, S. Ruiz, et al. 2021. Significance of root hairs for plant performance under contrasting field conditions and water deficit. *Ann. Bot.* 128(1): 1–16. doi: 10.1093/aob/mcaa181.
- Meunier, F., A. Heymans, X. Draye, V. Couvreur, M. Javaux, et al. 2020. MARSHAL, a novel tool for virtual phenotyping of maize root system hydraulic architectures. *In Silico Plants* 2(1): 1–15. doi: 10.1093/insilicoplants/diz012.
- Meunier, F., M. Zarebanadkouki, M.A. Ahmed, A. Carminati, V. Couvreur, et al. 2018. Hydraulic conductivity of soil-grown lupine and maize unbranched roots and maize root-shoot junctions. *J. Plant Physiol.* 227(February): 31–44. doi: 10.1016/j.jplph.2017.12.019.
- Morandage, S., J. Vanderborght, M. Zörner, G. Cai, D. Leitner, et al. 2021. Root architecture development

- in stony soils. *Vadose Zo. J.* (April): 1–17. doi: 10.1002/vzj2.20133.
- Müllers, Y., J.A. Postma, H. Poorter, and D. van Dusschoten. 2022. Stomatal conductance tracks soil-to-leaf hydraulic conductance in faba bean and maize during soil drying. *Plant Physiol.* doi: 10.1093/plphys/kiac422.
- Nguyen, T.H., M. Langensiepen, T. Gaiser, H. Webber, H. Ahrends, et al. 2022a. Responses of winter wheat and maize to varying soil moisture: From leaf to canopy. *Agric. For. Meteorol.* 314(December 2021): 108803. doi: 10.1016/j.agrformet.2021.108803.
- Nguyen, T.H., M. Langensiepen, H. Hueging, T. Gaiser, S.J. Seidel, et al. 2022b. Expansion and evaluation of two coupled root–shoot models in simulating CO₂ and H₂O fluxes and growth of maize. *Vadose Zo. J.* 21(3): 1–31. doi: 10.1002/vzj2.20181.
- Nguyen, T.H., M. Langensiepen, J. Vanderborgh, H. Hüging, C.M. Mboh, et al. 2020. Comparison of root water uptake models in simulating CO₂ and H₂O fluxes and growth of wheat. *Hydrol. Earth Syst. Sci.* (24): 4943–4969. doi: 10.5194/hess-24-4943-2020.
- Passioura, J.B., 2006. The perils of pot experiments. *Funct. Plant Biol.* 33 (12), 1075–1079. <https://doi.org/10.1071/FP06223>.
- Ranawana SRWMCJK, Siddique KHM, Palta JA et al (2021) Stomata coordinate with plant hydraulics to regulate transpiration response to vapour pressure deficit in wheat. *Functional Plant Biol* 48:839–850. <https://doi.org/10.1071/FP20392>
- Richards, R.A., G.J. Rebetzke, A.G. Condon, and A.F. van Herwaarden. 2002. Breeding Opportunities for Increasing the Efficiency of Water Use and Crop Yield in Temperate Cereals. *Crop Sci.* 42(1): 111–121. doi: 10.2135/cropsci2002.1110.
- Rodriguez-Dominguez, C.M., and T.J. Brodribb. 2019. Declining root water transport drives stomatal closure in olive under. *New Phytol.* 225: 126–134.
- Sinclair, T.R., and M.M. Ludlow. 1986. Influence of soil water supply on the plant water balance of four tropical grain legumes. *Aust. J. Plant Physiol.* 13: 329–341.
- Scharwies, J.D., and J.R. Dinneny. 2019. Water transport, perception, and response in plants. *J. Plant Res.* 132(3): 311–324. doi: 10.1007/s10265-019-01089-8.
- Schultz, H.R. 2003. Differences in hydraulic architecture account for near-isohydric and anisohydric behaviour of two field-grown *Vitis vinifera* L. cultivars during drought. *Plant, Cell Environ.* 26(8): 1393–1405. doi: 10.1046/j.1365-3040.2003.01064.x.
- Stadler, A., S. Rudolph, M. Kupisch, M. Langensiepen, J. van der Kruk, et al. 2015. Quantifying the effects of soil variability on crop growth using apparent soil electrical conductivity measurements. *Eur. J. Agron.* 64: 8–20. doi: 10.1016/j.eja.2014.12.004.
- Sulis, M., V. Couvreur, J. Keune, G. Cai, I. Trebs, et al. 2019. Incorporating a root water uptake model based on the hydraulic architecture approach in terrestrial systems simulations. *Agric. For. Meteorol.* 269–270: 28–45. doi: <https://doi.org/10.1016/j.agrformet.2019.01.034>.
- Sunita, C., T.R. Sinclair, C.D. Messina, and M. Cooper. 2014. Hydraulic conductance of maize hybrids differing in transpiration response to vapor pressure deficit. *Crop Sci.* 54(3): 1147–1152. doi: 10.2135/cropsci2013.05.0303.
- Tardieu, F., X. Draye, and M. Javaux. 2017. Root Water Uptake and Ideotypes of the Root System: Whole-

- Plant Controls Matter. *Vadose Zo. J.* 16(9): 0. doi: 10.2136/vzj2017.05.0107.
- Tardieu, F., and T. Simonneau. 1998. Variability among species of stomatal control under fluctuating soil water status and evaporative demand: modelling isohydric and anisohydric behaviours. *J. Exp. Bot.* 49(March): 419–432. doi: 10.1093/jxb/49.Special_Issue.419.
- Tardieu, F. 2016. Too many partners in root – shoot signals . Does hydraulics qualify as the only signal that feeds back over time for reliable stomatal. *New Phytol.* 212: 802–804.
- Trillo, N., and R.J. Fernández. 2005. Wheat plant hydraulic properties under prolonged experimental drought: Stronger decline in root-system conductance than in leaf area. *Plant Soil* 277(1–2): 277–284. doi: 10.1007/s11104-005-7493-5.
- Tsuda, M., and M.T. Tyree. 1997. Whole-plant hydraulic resistance and vulnerability segmentation in *Acer saccharinum*. *Tree Physiol.* (17): 351–357.
- Turner, N.C., E.D. Schulze, and T. Gollan. 1984. The responses of stomata and leaf gas exchange to vapour pressure deficits and soil water content - I. Species comparisons at high soil water contents. *Oecologia* 63(3): 338–342. doi: 10.1007/BF00390662.
- Tyree, M.T., E.L. Fiscus, S.D. Wullschlegel, and M.A. Dixon. 1986. Detection of Xylem Cavitation in Corn under Field Conditions. *Plant Physiol.* 82(2): 597–599. doi: 10.1104/pp.82.2.597.
- Vadez, V. 2014. Root hydraulics : The forgotten side of roots in drought adaptation. *F. Crop. Res.* 165: 15–24.
- Vadez, V., S. Choudhary, J. Kholová, C.T. Hash, R. Srivastava, et al. 2021. Transpiration efficiency: Insights from comparisons of C4cereal species. *J. Exp. Bot.* 72(14): 5221–5234. doi: 10.1093/jxb/erab251.
- Vanderborght, J., V. Couvreur, F. Meunier, A. Schnepf, H. Vereecken, et al. 2021. From hydraulic root architecture models to macroscopic representations of root hydraulics in soil water flow and land surface models. *Hydrol. Earth Syst. Sci.* 25(9): 4835–4860. doi: 10.5194/hess-25-4835-2021.
- Vanderborght, J., A. Graf, C. Steenpass, B. Scharnagl, N. Prolingheuer, et al. 2010. Within-Field Variability of Bare Soil Evapora Θ on Derived from Eddy Covariance Measurements. *Vadose Zo. J.* 9: 943–954. doi: 10.2136/vzj2009.0159.
- Vereecken, H., A. Schnepf, J.W. Hopmans, M. Javaux, D. Or, et al. 2016. Modeling Soil Processes: Review, Key Challenges, and New Perspectives. *Vadose Zo. J.* 15(5): vzj2015.09.0131. doi: 10.2136/vzj2015.09.0131.
- Vetterlein, D., M. Phalempin, E. Lippold, S. Schlüter, S. Schreiter, et al. 2022. Root hairs matter at field scale for maize shoot growth and nutrient uptake, but root trait plasticity is primarily triggered by texture and drought. *Plant Soil* 478(1–2): 119–141. doi: 10.1007/s11104-022-05434-0.
- Vitale, L., P. Di Tommasi, C. Arena, A. Fierro, A. Virzo De Santo, et al. 2007. Effects of water stress on gas exchange of field grown *Zea mays* L. in Southern Italy: An analysis at canopy and leaf level. *Acta Physiol. Plant.* 29(4): 317–326. doi: 10.1007/s11738-007-0041-6.
- Wang, N., J. Gao, and S. Zhang. 2017. Overcompensation or limitation to photosynthesis and root hydraulic conductance altered by rehydration in seedlings of sorghum and maize. *Crop J.* 5(4): 337–344. doi: 10.1016/j.cj.2017.01.005.
- Weihermüller, L., Huisman, J. A., Lambot, S., Herbst, M., & Vereecken, H. (2007). Mapping the spatial variation of soil water content at the field scale with different ground penetrating radar techniques.

Journal of Hydrology, 340, 205–216. <https://doi.org/10.1016/j.jhydrol.2007.04.013>

Welcker, C., W. Sadok, G. Dignat, M. Renault, S. Salvi, et al. 2011. A common genetic determinism for sensitivities to soil water deficit and evaporative demand: Meta-analysis of quantitative trait loci and introgression lines of maize. *Plant Physiol.* 157(2): 718–729. doi: 10.1104/pp.111.176479.

Zhuang, J., Y. Jin, and T. Miyazaki. 2001. ESTIMATING WATER RETENTION CHARACTERISTIC FROM SOIL PARTICLE-SIZE DISTRIBUTION USING A NON-SIMILAR MEDIA CONCEPT. *Soil Sci.* 166(5). https://journals.lww.com/soilsci/Fulltext/2001/05000/ESTIMATING_WATER_RETENTION_CHARACTERISTIC_FROM.2.aspx.

Zwieniecki, M.A., P.J. Melcher, C.K. Boyce, L. Sack, and N.M. Holbrook. 2002. Hydraulic architecture of leaf venation in *Laurus nobilis* L. *Plant, Cell Environ.* 25(11): 1445–1450. doi: 10.1046/j.1365-3040.2002.00922.x.

Author contribution

Huu Thuy Nguyen, Thomas Gaiser, Jan Vanderborght, and Frank Ewert: Conceptualization; Huu Thuy Nguyen, and Hubert Hüging: Data curation and data quality check (aboveground measurements); Lena Lärm, Felix Bauer, Anja Klotzsche, Jan Vanderborght, and Andrea Schnepf: data curation and data quality check (belowground measurements); Huu Thuy Nguyen: Formal data analysis and visualization; Thomas Gaiser, Jan Vanderborght, Andrea Schnepf, and Frank Ewert: Funding acquisition & Project administration; Huu Thuy Nguyen: writing – original draft; all authors: review, editing, and finalizing the manuscript.

Competing interests

This manuscript has not been published and is not under consideration for publication in any other journal. All authors agreed and approved the manuscript and its submission to this journal. We declare there is no conflict of interest.

Code/Data availability

The meteorological data were collected from a weather station in Selhausen (Germany) which belongs to the TERENO network of terrestrial observatories. Weather data are freely available from the TERENO data portal (<https://www.tereno.net/ddp/dispatch?searchparams=freetext-Selhausen>, last access: October 2020) (TERENO, 2020). The data which were obtained from the minirhizotron facilities (under- and aboveground) are available from the corresponding author on reasonable requests.